JOURNAL OF NEUROPHYSIOLOGY
Vol. 64, No. 2, August 1990. *Printed in U.S.A.*

Gaze Control in the Cat: Studies and Modeling of the Coupling Between Orienting Eye and Head Movements in Different Behavioral Tasks

DANIEL GUITTON, DOUGLAS P. MUNOZ, AND HENRIETTA L. GALIANA
Montreal Neurological Institute and Departments of Neurology and Neurosurgery and Biomedical Engineering, McGill University, Montreal, Quebec H3A 2T5, Canada

SUMMARY AND CONCLUSIONS

1. Orienting movements, consisting of coordinated eye and head displacements, direct the visual axis to the source of a sensory stimulus. A recent hypothesis suggests that the CNS may control gaze position (gaze = eye-relative-to-space = eye-relative-to-head + head-relative-to-space) by the use of a feedback circuit wherein an internally derived representation of gaze motor error drives both eye and head premotor circuits. In this paper we examine the effect of behavioral task on the individual and summed trajectories of horizontal eye- and head-orienting movements to gain more insight into how the eyes and head are coupled and controlled in different behavioral situations.

2. Cats whose heads were either restrained (head-fixed) or unrestrained (head-free) were trained to make orienting movements of any desired amplitude in a simple cat-and-mouse game we call the *barrier paradigm.* A rectangular opaque barrier was placed in front of the hungry animal who either oriented to a food target that was visible to one side of the barrier or oriented to a location on an edge of the barrier where it predicted the target would reappear from behind the barrier.

3. The dynamics (e.g., maximum velocity) and duration of eye- and head-orienting movements were affected by the task. Saccadic eye movements (head-fixed) elicited by the *visible target* attained greater velocity and had shorter durations than comparable amplitude saccades directed toward the *predicted target.* A similar observation has been made in human and monkey. In addition, when the head was unrestrained both the eye and head movements (and therefore gaze movements) were faster and shorter in the visible- compared with the predicted-target conditions. Nevertheless, the relative contributions of the eye and head to the overall gaze displacement remained task independent: i.e., the distance traveled by the eye and head movements was determined by the size of the gaze shift only. This relationship was maintained because the velocities of the eye and head movements covaried in the different behavioral situations. Gaze-velocity profiles also had characteristic shapes that were dependent on task. In the predicted-target condition these profiles tended to have flattened peaks, whereas when the target was visible the peaks were sharper.

4. Presentation of a visual cue (e.g., reappearance of food target) immediately before (<50 ms) the onset of a gaze shift to a predicted target triggered a midflight increase in first the eye- and, after ~20 ms, the head-movement velocity. Such sudden reaccelerations of the eye and head during a gaze shift suggested an on-line modification in the neural controller signals driving the movement, whereon signals of visual origin were superimposed on those provided by predictive elements.

5. Onset of head movement often preceded eye movement in behavioral conditions involving prediction and/or absence of attentive fixation. However, this initial head motion was slow and did not significantly contribute to the overall head displacement. Its effect on gaze was nulled by compensatory eye rotation. The head usually reaccelerated 20–30 ms after onset of the saccadic eye movement (i.e., onset of gaze saccade). This delay between eye and head accelerations may be accounted for by the greater inertia of the head because signals initiating the rapid eye and head accelerations probably reach the extraocular and neck muscles at about the same time.

6. In a typical head-free gaze shift the shapes of the head-velocity and -acceleration profiles closely resembled those of the eye-position and -velocity profiles, respectively. This was particularly striking during the ocular saccade, where eye velocity and head acceleration increased and decreased together. Near the end of a gaze shift, the eye began to counterrotate in the orbit (i.e., negative eye velocity) while the head decelerated. Such close links between the eye and head motor systems suggest that they share common driver signals.

7. A feedback model with the use of gaze motor error as the driver signal is presented wherein the controller signal sent to the eye plant also summates with a gaze error signal to drive the head. Computer simulations of the model produced trajectories of eye- and head-orienting movements that were very similar to those triggered naturally by cat. The model furthermore accounts for the influence of tectoreticulospinal (TRS) cell discharges on gaze control and predicts new gaze-related discharge properties of "oculomotor" brain stem neurons.

INTRODUCTION

In *head-restrained* (to be called "head-fixed") human, monkey, and cat, the tonic level of electromyographic (EMG) activity in many dorsal neck muscles can be modulated in relation to the position of the eye in the orbit. For example, as the eye moves progressively more in one direction there can be a concomitant tonic increase in the activity of ipsilateral neck muscles that participate in driving the head in that same direction (André-Dehays et al. 1988; Guitton et al. 1980; Lestienne et al. 1984; Roucoux et al. 1982; Vidal et al. 1982). In addition to this tonic component there is evidence that phasic bursts of neck EMG activity can accompany saccades (Berthoz and Grantyn 1986; Bizzi et al. 1971; Fuller 1980; Grantyn and Berthoz 1987).

Much of this evidence, obtained in head-fixed animals, suggests the existence of common driver signals to the eye and head motor systems. How this coupling expresses itself

in the subject whose head is unrestrained (*head-free*) is not well understood, and the aim of this paper is to provide more insight into this mechanism.

Many characteristics of head-free gaze shifts (gaze = eye-relative-to-space = eye-relative-to-head + head-relative-to-space) have been described for cat (Blakemore and Donaghy 1980; Collewijn 1977; Fuller et al. 1983; Guitton et al. 1984), monkey (Bizzi 1981, Bizzi et al. 1971, 1972; Morasso et al. 1973; Tomlinson unpublished observations; Tomlinson and Bahra 1986a,b; Whittington et al. 1981), and human (Barnes 1979; Funk and Anderson 1977; Gresty 1974; Guitton and Volle 1987; Laurutis and Robinson 1986; Zangemeister and Stark 1982a,b). A broad mosaic of movement strategies is possible. Saccadic eye and head movements can either be highly synchronized (e.g., Guitton et al. 1984; Guitton and Volle 1987) or can be initiated at different times relative to one another (e.g., Melvill Jones et al. 1988; Zangemeister and Stark 1982a,b). The manner in which the nervous system modulates the degree of coupling between eye and head is an intriguing question.

Two neural structures—the frontal eye fields (FEF) and the superior colliculus (SC)—have been extensively implicated in the control of gaze in the head-fixed condition. At least in cat these structures appear also to be involved in the control of gaze when the head is unrestrained (Guitton 1981; Guitton et al. 1980, Guitton and Mandl 1978a,b; Munoz 1988; Munoz and Guitton 1985, 1986, 1989a,b, and unpublished observations; Roucoux et al. 1980). A fascinating feature of the collicular output in cat and monkey is its profuse collateralization (Grantyn and Berthoz 1987; Grantyn and Grantyn 1982; Grantyn et al. 1987, 1988; Moschovakis and Karabelas 1985, Moschovakis et al. 1988a,b). Both tectoreticulospinal neurons (TRSNs) and reticulospinal neurons (RSNs) that receive monosynaptic collicular input send collaterals to both oculomotor and head motor circuits thereby providing an apparent substrate for the synchronization of eye and head movements during a gaze shift. The fact that the eye and head sometimes are not synchronized attests to the presence of overriding circuits that are even less well understood than the circuits responsible for the synchrony. The tectoreticulospinal (TRS) system is an important element in producing synchrony, and a study of this system in the head-free cat is the subject of subsequent papers (Munoz and Guitton unpublished observations).

To gain more insight into the mechanisms underlying eye-head coupling, such as whether or not there is a common driver signal, it is useful to compare gaze shifts having similar amplitudes but different trajectories. In this paper we first determine the behavioral paradigms that permit this. In human and monkey head-fixed saccades made to predicted and remembered targets are slower and have differently shaped velocity profiles than saccades made to targets that are visible (Becker and Fuchs 1969; Bon and Lucchetti 1988; Hikosaka and Wurtz 1985a; Sharpe et al. 1975; Smit and Van Gisbergen 1989, Smit et al. 1987). These differences in motor output can be attributed to the fact that saccades to either remembered or predicted targets may be controlled by signals flowing from the FEF to the SC and brainstem premotor circuitry via direct and indirect pathways (Bruce and Goldberg 1985; Hikosaka and Sakamoto 1986; Hikosaka and Wurtz 1983a–d, 1985a,b; Huerta et al. 1986; Leichnetz 1981; Segraves and Goldberg 1987), whereas visually triggered saccades may be controlled via the inferior parietal lobule and occipital cortical inputs to the SC (Keating and Gooley 1988; Pierrot-Deseilligny et al. 1987). It is of interest to extrapolate these ideas to the head-free condition and to determine whether differences in "motor set" affect in the same way both the eye and head trajectories.

From our observations the hypothesis emerges that head motion is controlled by two signals: one is the pulse signal that drives the eye saccade, and the other is a lower gain gaze-control signal. We will propose a model of gaze control that incorporates not only the coupling between eye and head motor systems but also some important anatomic pathways such as the projections of TRSNs to both the eye and head motor circuitry. No working model yet exists that treats gaze control in the head-free condition. Many models of the system have calculated eye and gaze trajectories with the use of a priori imposed head trajectories rather than deriving the head response from the model itself (Guitton et al. 1984; Laurutis and Robinson 1986; Pélisson et al. 1988; Tomlinson 1990). Other models have been essentially conceptual schemata whose function and parameters have not been adequately explored (Guitton 1988, Guitton and Volle 1987).

The behavioral observations and the model presented in this paper will be of considerable importance when interpreting the signals recorded from TRSNs to be described in subsequent papers (Munoz and Guitton unpublished observations).

A preliminary report of the data presented here has appeared elsewhere (Galiana et al. 1990; Guitton and Munoz 1988).

METHODS

The data described in this paper were obtained from four alert, trained cats that had previously been prepared for the eventual chronic recording of electrophysiologically identified tectoreticular neurons (TRNs) (Munoz and Guitton unpublished observations). Stimulating electrodes were placed in the predorsal bundle of these animals. One cat (*Q*) had 30 fine flexible 25-μm wires implanted in each SC for the purpose of recording TRNs. This paper will show that there were no fundamental behavioral differences between the implanted animals. When compared with previous experiments performed on cats that were not implanted with electrodes (Guitton et al. 1984), the present observations will show that the gaze-control system of our animals was normal.

General methods

The positions of gaze, head, and target each were measured relative to space with the search-coil-in-magnetic-field technique (Robinson 1963). The target-coil signal was used primarily as an event detector (see below). Details of the system, as well as procedures used in calibrating the gaze- and head-position signals and in calculating the position of the visual axis relative to the head (to be referred to as "eye") have been reported previously (Guitton et al. 1984). Briefly, the animals were prepared with the use of sterile surgical procedures performed under barbiturate anesthesia. A head implant was created with dental acrylic and anchored to the skull with four to six permanently implanted stainless steel bolts.

Coils (19 mm diam) consisting of three turns of stainless steel wire (21 strands, Teflon insulated) were sutured to the sclera of one or both eyes, forward of the extraocular muscle insertions. The wire leads passed subcutaneously to the acrylic implant. An attachment for a similar coil of wire that monitored head position was embedded in the implant. A thin stainless steel U-shaped crown was embedded in the posterior perimeter of the implant. The cat's head could be immobilized by securing this crown to a rigid immobile stand mounted on the recording table. This restraining system was designed so that the cat's head could be simply and quickly released.

Each cat's gaze- and head-coil signals were then calibrated by oscillating the field-coil arrangement horizontally about the earth-fixed animal. The field-coil angular deviation was obtained from a potentiometer. The head-, gaze-, and field-coil–potentiometer signals were stored on FM tape. During off-line computer analysis (see below) a linearized calibration was obtained by selecting a saccade-free segment of data and storing, in a separate calibration file, a look-up table of head- and gaze-coil signals versus the known field-coil angular deviation determined from the potentiometer signal. During analysis of experimental data, gaze and head signals were transformed into known angular deviations. The head-coil signal was subtracted from the gaze-coil signal to obtain the eye signal.

Behavioral paradigms

Behavioral paradigms were designed to obtain rapidly and reliably a large number of coordinated eye-head displacements having a wide range of amplitudes and directions that the experimenter could control with minimal training in an alert animal behaving as naturally as possible. To conduct an experiment, a cat was first placed in a loosely fitting cloth bag and then into a box that gently restrained the body but permitted unrestricted horizontal head movements of up to 90° to the left or right. Upward head movements were unrestricted whereas downward head movements were limited so that the horizontal stereotaxic plane, if it were imagined to move with the cat's head, could go no further than 60° below the earth's horizontal. A rectangular opaque barrier was placed 40 cm in front of the hungry animal and a food target, consisting of a small portion of moist, pureed cat food placed on a small plastic spoon, was either hidden behind the barrier or protruded from one side. Figure 1 illustrates in *schematic* form the various natural behavioral situations that could be elicited with this simple hide-and-seek game.

The *top* portion of every section shows the cat in different phases of a horizontal-orienting gaze shift in response to horizontal displacements of the food target relative to the barrier. The *bottom* part of each section shows a hypothetical recording of the

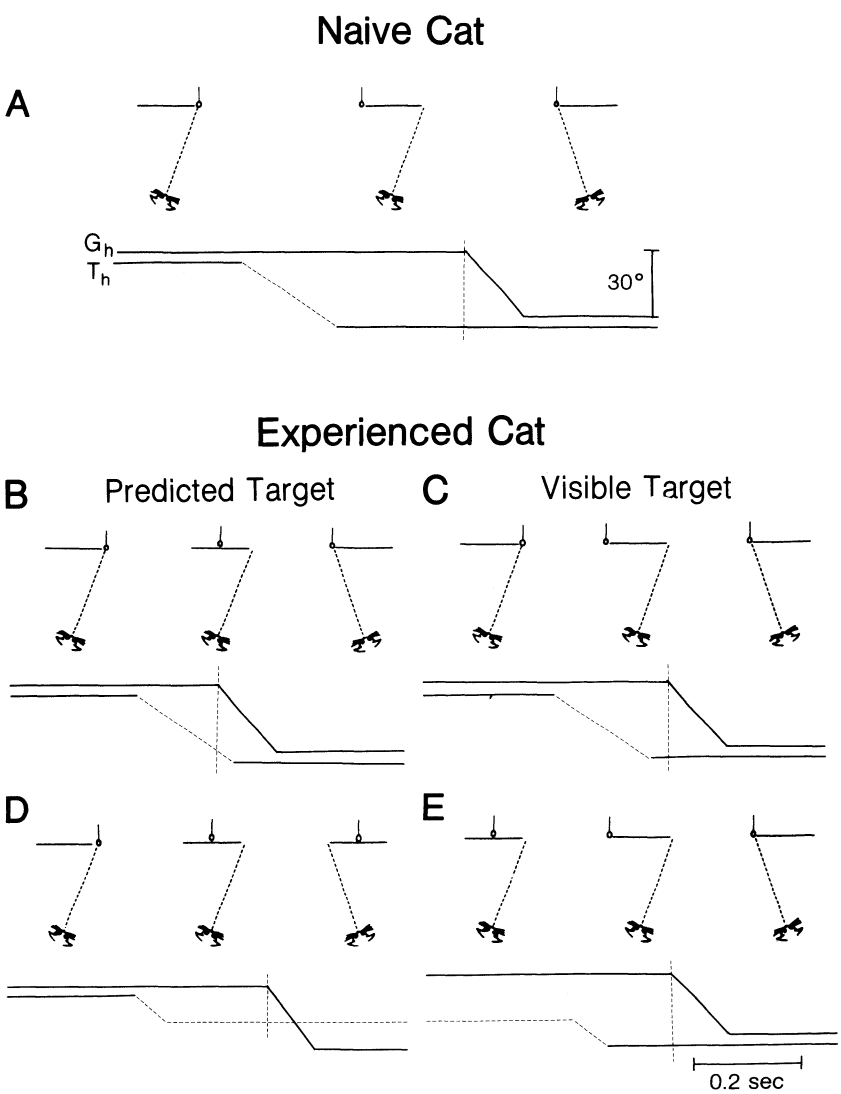

FIG. 1. Schematic examples of different food-target displacements and orienting movements in the barrier paradigm. *Top* portion of each section shows the alignment of the cat's visual axis in relation to the barrier and food target. *Bottom* part of each section illustrates a hypothetical recording of the horizontal target- (T_h) and gaze- (G_h) position traces. Upward and downward trace deflections correspond to rightward and leftward movements, respectively. Target-position trace is dashed when the target was hidden from the cat's view behind the barrier. Vertical dashed line denotes onset of the orienting movement. *A–C*: target is moved from the right side of the barrier to the left, and the cat orients left at different latencies relative to target reappearance. Gaze shifts initiated after the target reappeared (*A* and *C*) are directed toward the visible target. Gaze shifts triggered before target reappearance (*B*) are directed toward the predicted target. Naive cat does not make predictive movements, and when the target disappears from one side and reappears on the other, latency of a gaze shift is longer. *D*: target is moved from the right side of the barrier to behind, and the cat orients to the predicted target. *E*: target, initially hidden behind the barrier, suddenly appears on the left, and cat orients to the visible target.

horizontal-target (T_h) and gaze-position (G_h) traces. In these schematics and all subsequent real-position records, upward and downward deflections of a trace correspond to rightward and leftward movements, respectively. The target-position trace in Fig. 1 and all subsequent figures is dashed when the food target was hidden from the cat's view by the barrier. A trial began with the food target being protruded out and held visible for an arbitrary time, randomly from any one of the four sides of the barrier. For example, in Fig. 1*A* the trial begins with the food target appearing on the right side of the barrier. The animal aligned its head and visual axes on the target. At an unsuspected time the food was then moved quickly behind the barrier and reappeared on the other side, whereupon, after a visual reaction time of ~200 ms, the animal quickly reoriented its visual axis onto the target in the new position and was rewarded with food. Barrier width and orientation were adjustable to have the cat generate gaze shifts with a wide variety of amplitudes and directions. Cats were trained on this task before surgery.

The animals quickly learned that disappearance of the food target from one side of the barrier meant future reappearance on the other side. Consequently, in the experienced animal it was rare to observe many successive movement patterns such as that seen in Fig. 1*A*. The more frequent responses are shown schematically in Fig. 1, *B* and *C*, where, after target disappearance from the right side of the barrier, the trained cat anticipated target reappearance on the left side. In Fig. 1*B* the animal began orienting before the target was visible on the left. In this situation the cat directed its orienting movement to a *predicted* target (i.e., to the location where it expected the target to reappear). On some trials, as in Fig. 1*A*, the gaze shift was triggered after the food reappeared and was therefore directed toward a *visible* target (Fig. 1*C*).

In Fig. 1*D* the food target was moved behind the barrier but did not reappear on the left; nevertheless, the trained animal generated an orienting movement to the left side of the barrier where it expected the target would reappear. This is another example of a gaze shift made to a predicted target. If the target remained hidden the aroused animal began looking to and fro from one side of the barrier to the other in anticipation of the target's reappearance. In Fig. 1*E*, after being hidden for a variable length of time, the food target suddenly reappeared unexpectedly on the left side of the barrier, and the animal oriented to the now visible target.

Although the food target was displaced manually, we attempted to make the trajectories of the target as it moved either from one side of the barrier to the other or from behind the middle of the barrier to one side, as highly stereotyped as possible. This was facilitated by monitoring the target's position with the use of the search-coil technique. A coil of wire was mounted on the spoon's handle such that the axes of the handle and coil were coextensive. We discovered empirically that translational motion of the spoon from one side of the barrier to the other yielded a smooth signal linearly related to spoon position. This was presumably because the spoon's search coil was off the field-coil center.

When the target was visible to either side of the barrier, it was extended 2–3 cm beyond the edge of the barrier. In a trial the cat did not know beforehand whether he would be rewarded by the spoon advancing toward him or whether the spoon would disappear behind the barrier. Consequently, unintentional small movements of the spoon did not appear to constitute cues to orient. This was verified by assessing the latency of the orienting gaze shifts relative to target disappearance. The stereotyped trajectory of the target allowed us to estimate the time at which it disappeared behind the barrier. In one cat the mean latency at which gaze shifts were triggered by the disappearing target was 220 ms (SD ± 140, $n = 33$). This time is comparable with that observed in primates making saccades to remembered targets after extinction of a fixation point (Hikosaka and Wurtz 1983c).

The reliability of our behavioral technique was further evaluated by estimating the latency of orienting responses to the sudden appearance of the food target on one side of the barrier. The time was measured as 145 ms (SD ± 55, $n = 27$). To verify that this estimate was correct, one of the cats was also trained to orient to a light-emitting diode (LED) in return for a food reward. Training procedures have been previously reported (Guitton et al. 1984; Munoz 1988). Briefly, a LED was attached, say, to the left edge of the same opaque barrier as described above. The LED was illuminated when the food target was hidden behind the barrier and the searching cat was looking to the opposite side, before an eventual return movement to the left. Even naive animals frequently oriented to the LED in this condition and when rewarded readily learned the task. With the use of this procedure the estimated latency of a head-free orienting response to the precisely measured LED onset was 162 ms (SD ± 52, $n = 35$), a value not significantly different from the 145-ms latency in the barrier paradigm. Such short reaction times may be related both to the absence of fixation signals when the food target was hidden (Fischer and Boch 1983) and the cat being in a searching mode.

Data storage and analysis

Horizontal and vertical gaze-, head-, and food-target positions were recorded on FM tape. At a later time selected portions of the experiment were played back and sampled onto a computer. Depending on the number of channels being sampled, relevant signals were low-pass filtered at 250 Hz (−3dB) and digitized at 500 or 1,000 Hz. During off-line analysis the orienting movements were viewed on a large-screen oscilloscope. A semiautomatic analysis software package, graciously provided by Dr. R. M. Douglas (Dept. Ophthalmology, University of British Columbia) was used in which the experimenter placed cursors at the onset and termination of selected movements. Gaze, head, and eye characteristics such as amplitude, maximum velocity, and duration were automatically measured and stored in separate analysis files. Velocity and acceleration traces were derived from position traces by calculating the instantaneous slope across five data points. This procedure led to some misalignment in the velocity and acceleration traces. For example, when sampling at 1kHz with five-point differentiation, a step change in position at time $t = 0$ leads to a spread in the velocity profile between -2 ms $< t < 2$ ms. When calculating latencies from velocity profiles, the highest sampling rate of position was used (1kHz) and a 2-ms correction was applied. Position, velocity, and acceleration traces from selected movements could be aligned with any observable event (e.g., LED onset, peak gaze velocity, etc.) and rank ordered according to any chosen criteria (e.g., response latency, gaze amplitude, etc.).

RESULTS

The characteristics of only horizontally directed eye-head orienting movements are considered in this paper. The range of vertical component that was tolerated was ±10°. We will first compare the metrics of eye, head, and gaze movements made in the barrier paradigm (Fig. 1) by cats that oriented to visible and predicted food targets in both the head-fixed and head-free conditions. Because the experiments yielded very similar results in the four cats, detailed results from only one animal will be presented. Summary figures and a Table will compare all cats.

Characteristics of movements to predicted and visible targets

Figure 2 illustrates some general characteristics of orienting movements directed toward predicted and visible

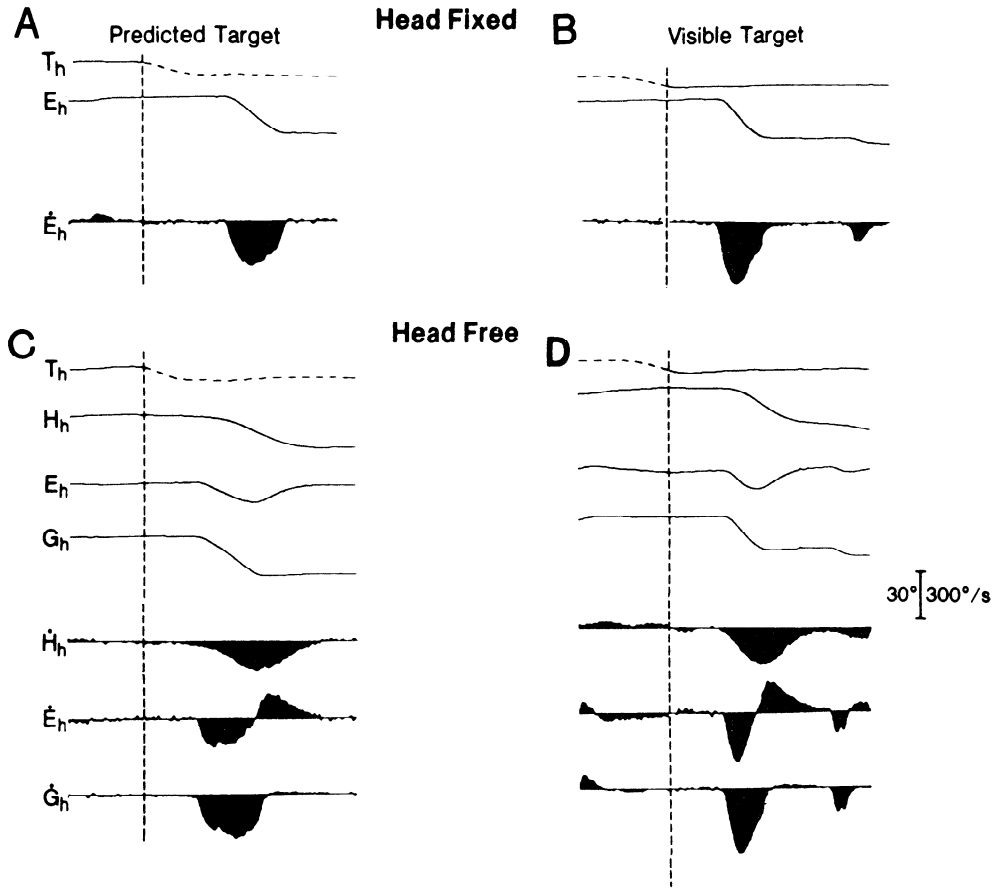

FIG. 2. Predicted-target condition: examples of the head-fixed (*A*) and head-free (*C*) cat orienting to a predicted target. Food target, initially visible to the right, is moved behind the barrier and, after a delay (200 ms, head-fixed; 165 ms, head-free), the cat orients left. Vertical dashed line denotes target disappearance. Visible-target condition: examples of head-fixed (*B*) and head-free (*D*) cat orienting to a visible target. Food target, initially hidden behind the barrier, suddenly appears on the left side, and after a delay (100 ms, head-fixed; 110 ms, head-free) the cat orients left. Vertical dashed line denotes target appearance. T_h, H_h, E_h, G_h: horizontal component of target, head, eye, and gaze motion. Dots over symbols indicate velocity.

targets. The data presented in this figure were collected from a single recording session with *cat H*. Movements directed toward a predicted target were easily elicited by moving the food target, initially visible on one side of the barrier, to behind it (explained in Fig. 1*D*). Examples of such movements are illustrated for the head-fixed and head-free conditions in Fig. 2, *A* and *C*, respectively. After the target remained hidden behind the barrier for a variable length of time, it was moved quickly and arbitrarily to one side or the other, as explained schematically in Fig. 1*E*. An orienting response was triggered by the sudden appearance of the target. Examples of these types of movements to the visible target are shown in Fig. 2, *B* (head-fixed) and *D* (head-free).

There were consistent and notable differences in the shapes of the gaze-velocity profiles between the predicted- and visible-target conditions. The gaze-velocity profiles recorded in both conditions tended to be bell shaped, but the former (Fig. 2, *A* and *C*) had broad, blunt, or flat peaks compared with the latter (Fig. 2, *B* and *D*) whose peaks were more sharply pointed. For the same amplitude of gaze shift, the visually triggered movements were faster. (This is considered in greater detail below.) Of particular relevance to mechanisms of eye-head coupling, both eye and head movements were faster in the visible-target condition. These differences in the gaze-velocity profiles between the predicted- and visible-target conditions were present irrespective of the size of the gaze shift, more specifically, irrespective of whether the gaze shift was made to a target within or beyond the animal's oculomotor range (OMR). This is illustrated in Fig. 3, *A–D*, which compares, also for *cat H*, five movements of equal amplitude in the visible- and predicted-target conditions, respectively, with targets within (<25°, Fig. 3, *A* and *B*) and beyond (>25°, Fig. 3, *C* and *D*) the OMR. This cat consistently produced highly stereotyped movements in each condition. Note that peak velocities of gaze, eye, and head are lower in the predicted- than in the visible-target condition. Consequently, the duration of predictive movements are longer than visually triggered ones. Furthermore, in movements to predicted targets beyond the OMR, the approximately flat portion of maximum $\dot{G}_h$ occupies a proportionally longer interval within the overall gaze shift. A direct comparison between trajectories is made in Fig. 3, *E* and *F*, which shows the

superposition of position and velocity records of typical comparable amplitude gaze shifts made to the predicted (– – –) and visible (——) targets.

Amplitude-velocity and amplitude-duration relationships in the predictive- and visible-target conditions

To compare in a more quantitative manner the predicted- and visible-target modes, we present the characteristic "main-sequence" relations for eye movements in the head-fixed condition (Fig. 4, *A* and *E*) and for eye, head, and gaze movements in the head-free condition (Fig. 4, *B–D* and *F–H*). The data obtained from three cats were grouped into 5°-bins of movement amplitude. The mean and standard error are shown for each 5°-bin in both the predicted- (○, □, △) and visible- (●, ■, ▲) target conditions. Based on data discussed below with respect to Fig. 6, movements classified as being visually driven were made 50 ms or more after the target had appeared from behind the barrier. Orientations triggered in ambiguous situations such as those where there were midflight accelerations in the velocity profiles attributable to the influence of the visual target (e.g., Fig. 6, *B* and *F*) were not included in the analysis.

Figure 4, *A* and *D*, shows for three cats that the mean peak gaze velocity for a given amplitude of movement was generally higher when the target was visible compared with when it was predicted, irrespective of whether the head was fixed or free. The same observations apply to eye and head motion (Fig. 4, *B* and *C*). Data on head motion for *cat F* are not included because this animal tended to make multiple-step gaze shifts that were so closely linked that the distinction between adjacent head movements was frequently ambiguous. In general there were no statistically significant differences between the visible- and predicted-target conditions at the small eye and head amplitudes (marked by symbols over the abscissas).

In spite of the fact that frequent asymptotic termination of gaze and head movements made duration a noisier quantity to measure, the amplitude-duration relationships were compatible with the maximum velocity-versus-amplitude relations. Figure 4, *E–H*, shows that for a given amplitude the durations of head-fixed eye movements as

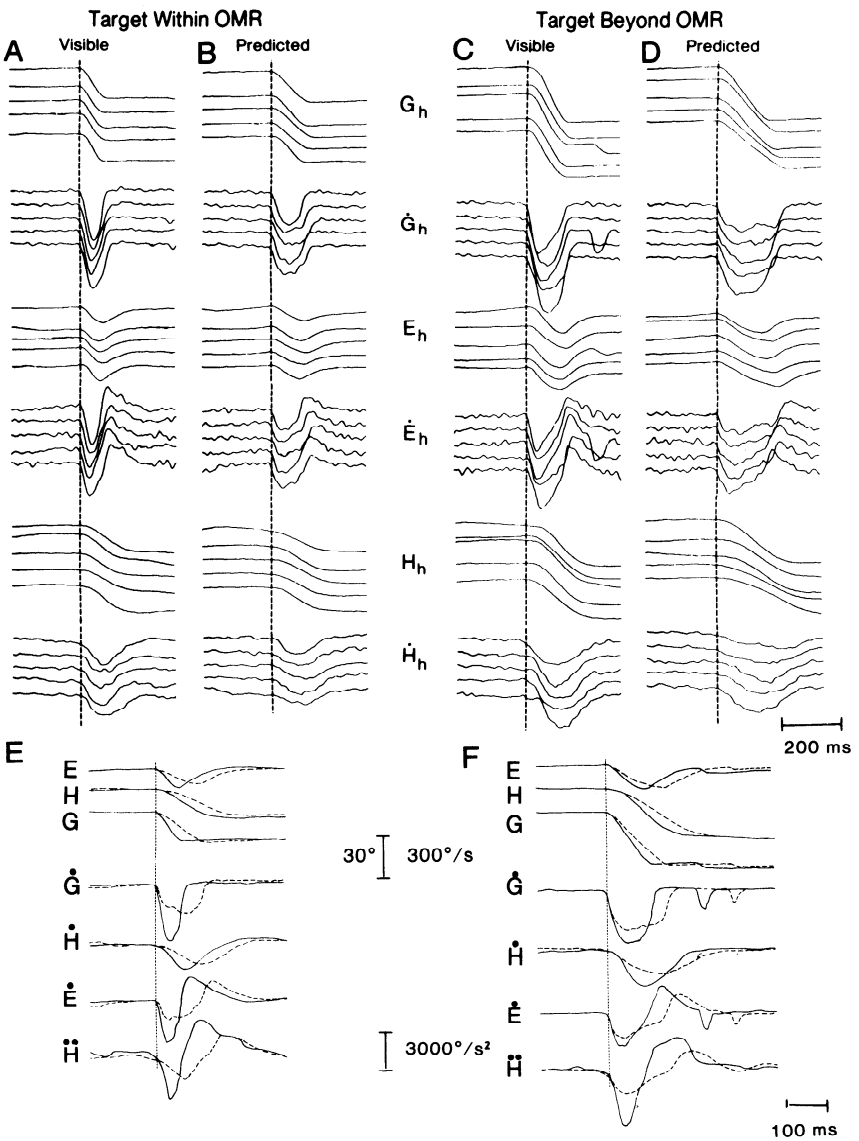

FIG. 3. Comparison of head-free orienting movements to visible (*A* and *C*) and predicted (*B* and *D*) targets located within (*A* and *B*) and beyond (*C* and *D*) the cat's oculomotor range (OMR). Shown in each section are 5 examples of corresponding position and velocity traces of gaze, eye, and head. Traces are aligned on the onset of gaze saccades that are marked by vertical dashed lines. *E* and *F*: comparison of position and velocity records of comparable amplitude movements made to the predicted (– – –) and visible (——) target. Traces are aligned on the onset of the gaze shift (denoted by vertical dashed lines). Also shown is the instantaneous head acceleration ($\ddot{H}$). *E*: target was located within the cat's OMR. *F*: target was beyond OMR. Symbols are as in Fig. 2.

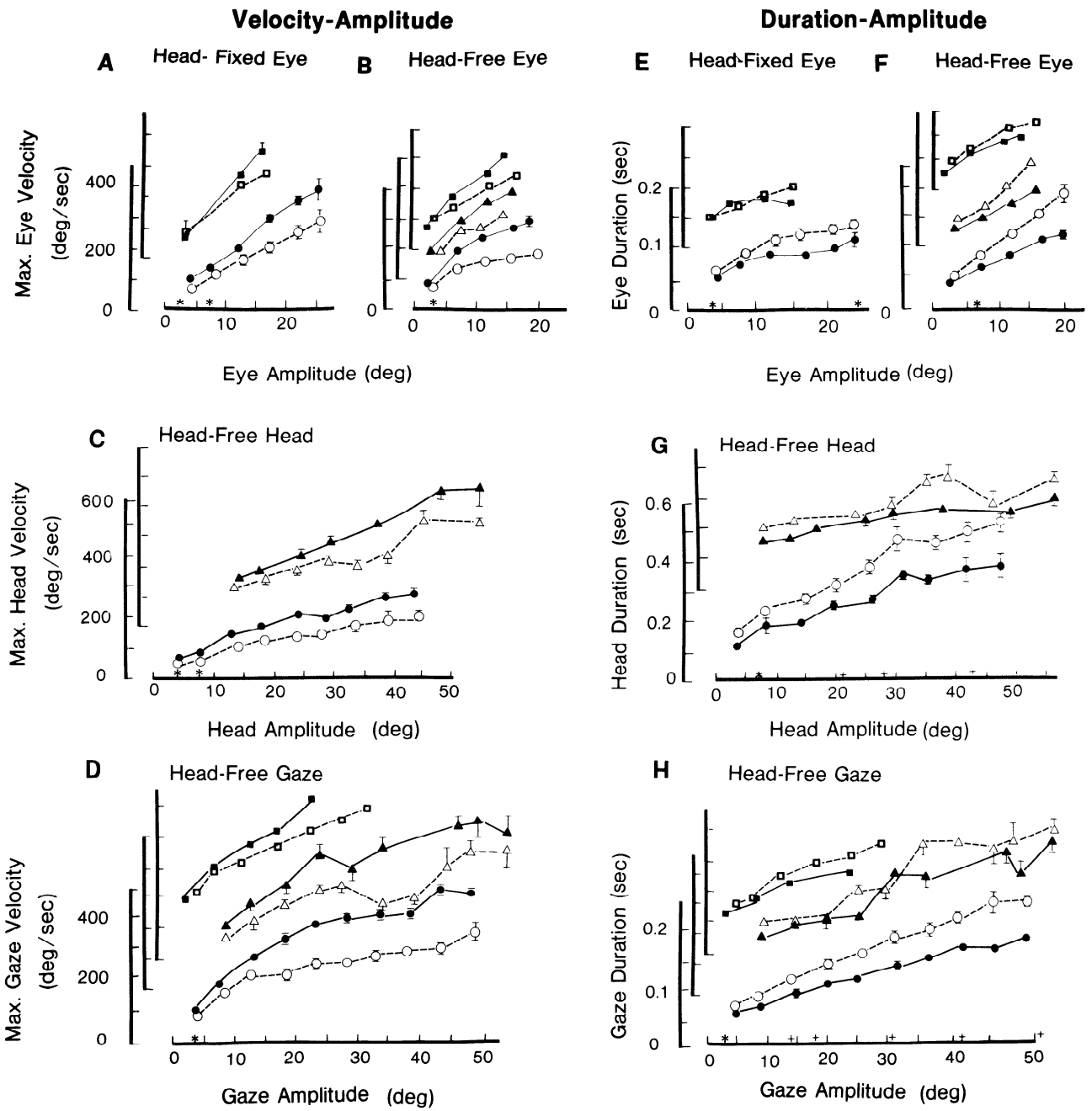

FIG. 4. Main-sequence relationships for 3 cats linking maximum velocity to amplitude (*A–D*) and duration to amplitude (*E–H*) for head-fixed eye (*A* and *E*) and head-free eye (*B* and *F*), head (*C* and *G*), and gaze (*D* and *H*) movements, comparing visible- (●, ■, ▲) and predicted- (○, □, △) target conditions. Data were grouped into 5°-bins and expressed as the mean ± SE (●, ○, *cat H*; ■, □, *cat F*; ▲, △, *cat Q*). Point-by-point statistical comparison was performed for all amplitudes of movement shown (*t* test, $P = 0.01$). Symbols lacking a vertical bar denote a standard error equal to or less than the size of the symbol. Asterisks, plus signs, and crosses above the abscissas denote those amplitudes where the difference between visible- and predicted-target conditions was not significant for *cats H, F*, and *Q*, respectively.

well as those of head-free eye, head, and gaze movements were generally shorter in the visible-target mode. Nonsignificant differences (symbols above the abscissas) occurred at small amplitudes of movement, save principally for *cat Q* (▲, △) where in the whole range differences between the durations in the two paradigms were less distinct.

Despite significant differences between the metrics of movements to predicted and visible targets there was little difference between the contributions of the eye movement to the overall gaze displacement in these two conditions (Fig. 5). The reason is that the eye and head velocities covaried in each condition such that at any point in the gaze shift the relative contribution of each to gaze remained about the same.

Visually evoked modifications to predictive trajectories

Some forms of target displacement were used in the barrier paradigm that produced gaze shifts in which the com-

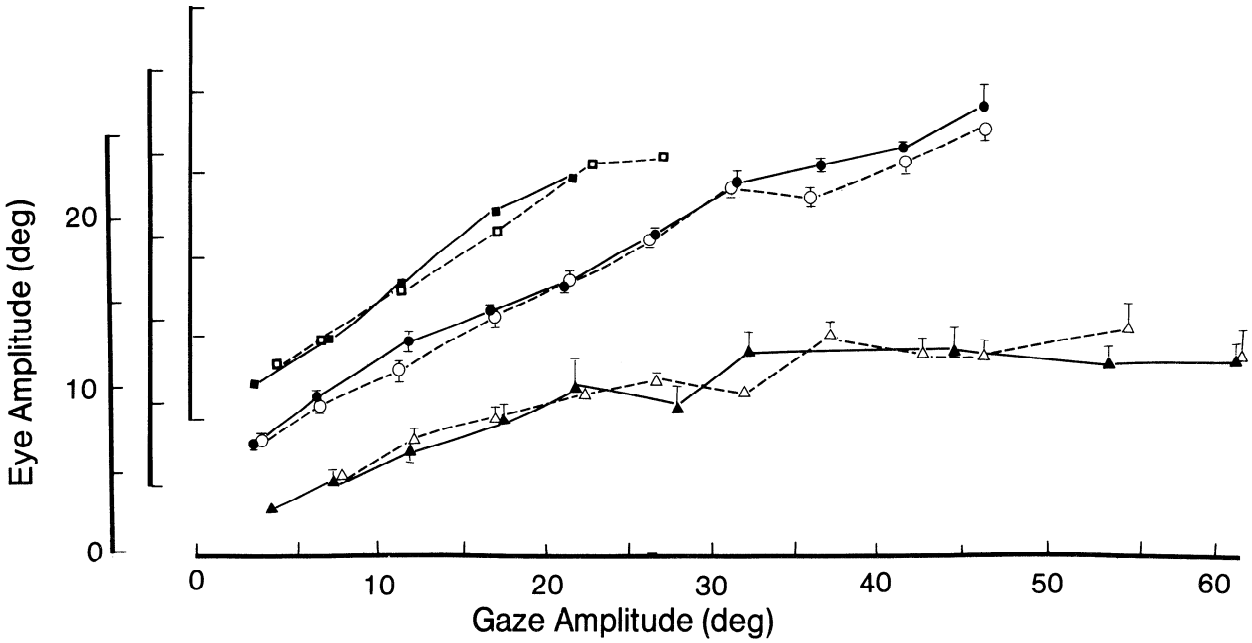

FIG. 5. Plot of eye amplitude versus gaze amplitude comparing movements to the visible (●, ■, ▲) and predicted (○, □, △) targets. Each of the 3 sets of lines represents data from 1 cat (●, ○, *cat H*; ■, □, *cat F*; and ▲, △, *cat Q*). Data were grouped into 5° bins of gaze amplitude and expressed as the mean ± SE.

bined effects of vision and prediction affected a given movement trajectory. As discussed with respect to Fig. 1, *A–C*, when the food target, initially visible to one side of the barrier, was moved with a rapid continuous motion behind the barrier and reappeared on the other side, there resulted movements with quite variable latencies relative to the time at which the target reappeared. Figure 6 shows examples of such movements for *cat H* in the head-fixed and head-free conditions. The vertical dashed lines denote target reappearance and also denote *time 0* on the abscissa of Fig. 6, *D* and *H*, where histograms of the number of movements with specific latencies are shown.

The latency histograms show a continuum of responses ranging from ~100 ms before to 100 ms after the reappearance of the target. The letters appearing within the histograms mark the latency of the correspondingly labeled trials. Gaze shifts triggered before the target reappeared (Fig. 6, *A* and *E*) were clearly predictive and had blunt or flat-topped velocity profiles, even though the target usually reappeared during the execution of the movement. By comparison, gaze shifts of similar amplitude initiated at times as little as 50 ms after the target reappeared (Fig. 6, *C* and *G*) had greater peak velocities, shorter durations, and more sharply peaked velocity profiles, typical of movements to the visible target. The mean latency of visually triggered gaze shifts for the cat illustrated in this figure was ~150 ms. Yet, the metrics of such movements were indistinguishable from those made at much shorter latencies (~50 ms) when both predictive and visual cues were presented. One can explain these extremely short-latency visually triggered movements by the fact that, in the trained cat, some of the neural events necessary for the generation of a gaze shift had been started by the disappearance of the target and that its reappearance on the other side acted as an early trigger.

The role of target reappearance as an early trigger is best appreciated when considering movements that started <50 ms after target reappearance. During the gaze shift these

TABLE 1. *Times between eye and head movements*

Cat	Paradigm	Conditions	Mean Latency between Onsets of Eye and Head Movement, ms	Time to Reacceleration of Head After Onset of Eye Saccade, ms
H	Barrier	Predicted target	−16 ± 38 (75)*	31 ± 24 (28)
		Visible target	−4 ± 27 (66)	22 ± 14 (20)
		Modified trajectory		20 ± 2 (7)
Q	Barrier	Predicted target	−26 ± 22 (65)	19 ± 9 (28)
		Visible target	−19 ± 21 (31)	15 ± 7 (14)
S	Barrier	Predicted target	−35 ± 17 (34)	13 ± 11 (19)
		Visible target	−25 ± 15 (41)	13 ± 9 (21)
F	LED	LED on when food hidden behind barrier	−39 ± 27 (79)	22 ± 13 (38)

Values are means ± SD; total number of trials in parentheses. Latency is measured from onset of saccade; latency is negative when eye lags head and positive when eye leads head. *Significantly different from visible target condition (*t* test, $P < 0.05$). LED, light-emitting diode.

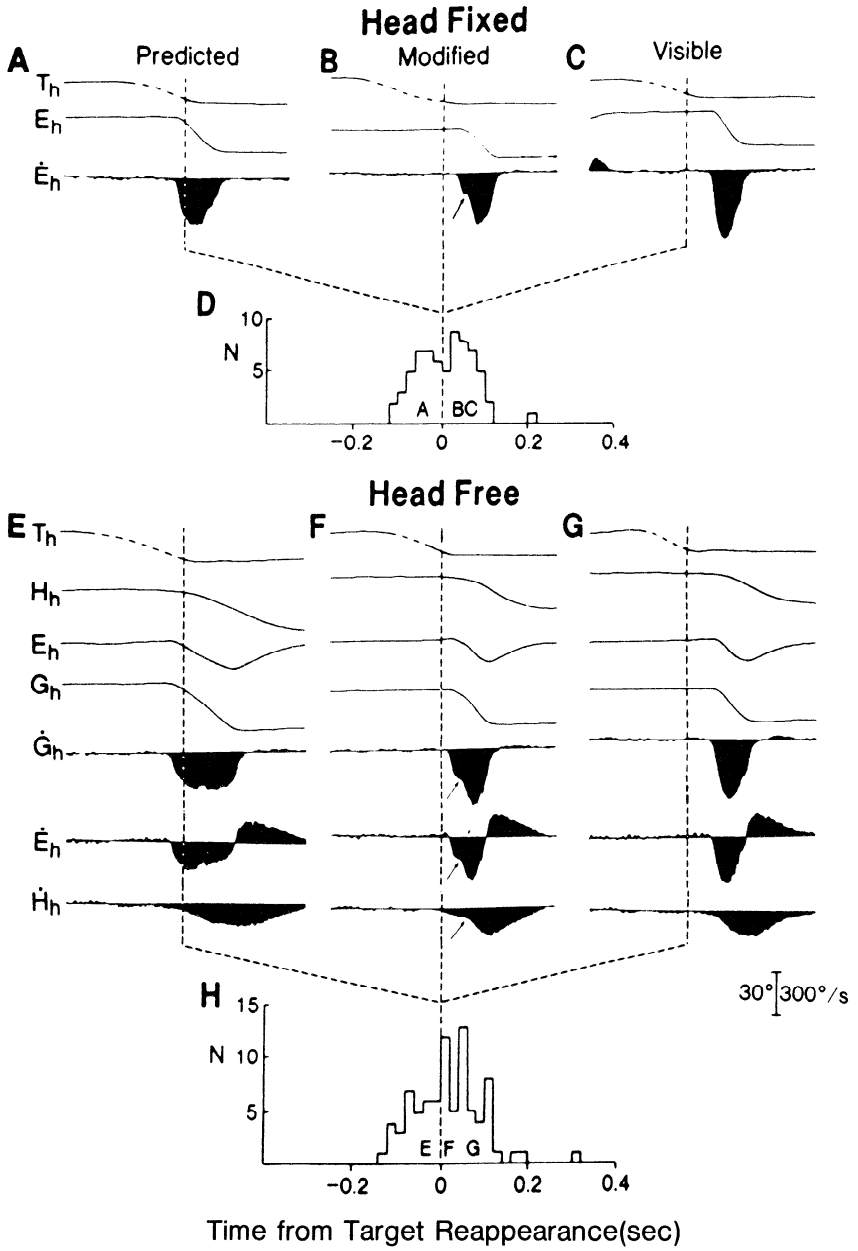

FIG. 6. Combination of predictive and visual cues trigger orienting responses in the head-fixed (*A–D*) and head-free (*E–H*) cat. Food target was moved from the right to the left side of the barrier. Vertical dashed lines denote target reappearance on the left side. Cat generated a leftward gaze shift either before (*A* and *E*) or after (*B, C, F*, and *G*) target reappearance on the left. Arrows point to the reacceleration in movement trajectories when gaze was initiated less than ~50 ms after target reappearance. Symbols are as in Fig. 2. *D* and *H*: histogram of response latencies aligned on target reappearance. Letters appearing within the histogram mark bins within which fall response latencies of trials illustrated above.

orienting responses had a sudden reacceleration that followed target reappearance by ~50–60 ms (Fig. 6, *B* and *F*). The notch in the gaze-velocity profile (denoted by the small arrows) appears to distinguish two separate processes. Before the notch the velocity profile had just begun to round-off and assume a shape characteristic of a movement to a predicted target. After the notch the $\dot{E}_h$ (head-fixed) and $\dot{G}_h$ (head-free) profiles assumed the high-velocity, sharply peaked profiles characteristic of visually triggered gaze shifts. Note that in the head-free condition (Fig. 6*F*), the modification in movement trajectory was observed in both the eye- ($\dot{E}_h$) and head- ($\dot{H}_h$) velocity profiles. In *cat H* where modified trajectories were extensively studied, the midflight reacceleration of the eye preceded that of the head by 20 ms (see Table 1). Such sudden accelerations of the eye and head during gaze shifts suggest an on-line modification in the neural controller signals to both eye and head, whereupon signals of visual origin are superimposed on those provided by the predictive elements. The time, 20 ms, is similar to the time to reacceleration of the head after the onset of a saccadic eye movement (Table 1). This characteristic of the common drive to the eye and head will be examined extensively in subsequent sections of this paper.

These results were verified in the LED paradigm, for which cats sometimes began to orient to the other side of the barrier before the LED was illuminated. This behavior occurred because the cat would frequently look to and fro to either side of the barrier in search of the hidden food. The LED occasionally came on immediately before these predictive orienting movements. In such trials the gaze-velocity profile had a notch marking a reacceleration of the visual axis in midflight such as illustrated above. The time between LED onset and gaze reacceleration was, as in the

barrier paradigm, ~50–60 ms. Because LED onset time was known precisely, these latencies provide strong support for the results obtained in the barrier paradigm.

Covariance of eye and head latencies

In a head-free gaze displacement, the onset of the gaze shift is normally synchronous with the initiation of the saccadic eye movement; the head usually begins moving either just before or after the onset of eye motion. In the former condition gaze is initially stabilized by the vestibulocular reflex (VOR).

The second column from the right in Table 1 summarizes for each of four cats the mean time between the onsets of eye and head movement (to be called "latency of eye-re-head") for the behavioral tasks used in this study. When in the barrier paradigm the orienting movement was made to the visible target, the mean latency of eye-re-head for the three cats tested was about −15 ms (eye lags head). By comparison, the mean latency of eye-re-head was −26 ms in the predicted-target condition. For *cat F* tested in the LED paradigm, the eye lagged the head on average by 39 ms.

Thus on average in all behavioral paradigms head motion slightly preceded eye motion. How does this observation link-up with our previous observation (Fig. 6, *B* and *F* and Table 1) that head acceleration was tightly coupled and followed eye acceleration? This question can best be answered by considering Fig. 7, which shows examples of gaze shifts of *cat F* in the LED paradigm. These results are illustrative because, as seen in Table 1, the average time by which the eye lagged the head was important in this paradigm. Note from the individual and mean head-velocity traces that initial head velocity followed LED onset by ~100 ms and rose very slowly until ~20 ms after the start of the eye motion at which point the head accelerated and the familiar head saccade occurred. For all cats and in all behavioral paradigms used in this study, the head, in about one third to one half of the trials, had a readily discernable reacceleration that followed the onset of the saccadic eye movement with a mean time across all cats of 20 ms (Table 1). An important conclusion from these results is that head motion is apparently driven by two processes: one that acts at short latency and produces a low acceleration and another coupled to eye motion that provides the kick responsible for the important head acceleration leading to the rapid head saccade. These ideas are formalized in the model presented in a subsequent section.

Further evidence for a common drive to the eye- and head-motor plants

Although slow head motion can precede saccade onset, the observations presented above show that the principal head displacement can be strongly coupled both in timing and speed to the saccadic eye movement. This is evidence that the eye and head share a common motor drive. It is of interest to consider further what effect such a hypothetical single motor command would have on eye and head motion.

The eyeball with its connective tissues and muscles, called the eye plant, constitutes a viscoelastic system. It is now well known that the forces controlling ocular rotation during a saccade are dominated by viscous elements (Robinson 1975, 1981). By comparison, greater head mass suggests that inertial forces dominate during rapid head movements (Zangemeister et al. 1981). These arguments suggest that, to a first approximation, a pulse sent to the extraocular muscles should control eye velocity whereas the same pulse sent to the head plant should determine head acceleration. Thus $\dot{E}$ and $\ddot{H}$, or E and $\dot{H}$, traces should resemble each other. This remarkable similarity was evident in Fig.

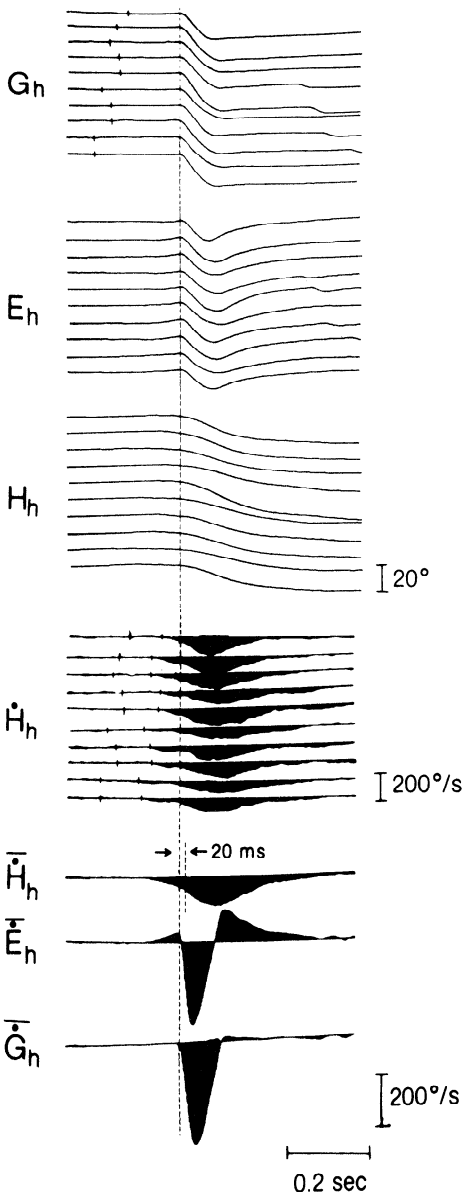

FIG. 7. Characteristics of 10 orienting movements to a LED in which head motion preceded onset of eye movement. Traces are aligned on onset of the gaze shift marked by the vertical dashed line. Symbols are as in Fig. 2. Horizontal bars over symbols indicate computer-averaged traces from the same 10 trials. Small vertical ticks on horizontal gaze-position traces denote LED onset. *Left* and *right* vertical tick marks on horizontal head-velocity traces denote LED onset and initiation of head motion, respectively. Note the relatively constant duration between these 2 events. Right-most short vertical dashed line intersecting the $\dot{H}_h$ trace marks the time of head reacceleration that follows onset of the saccadic eye movement.

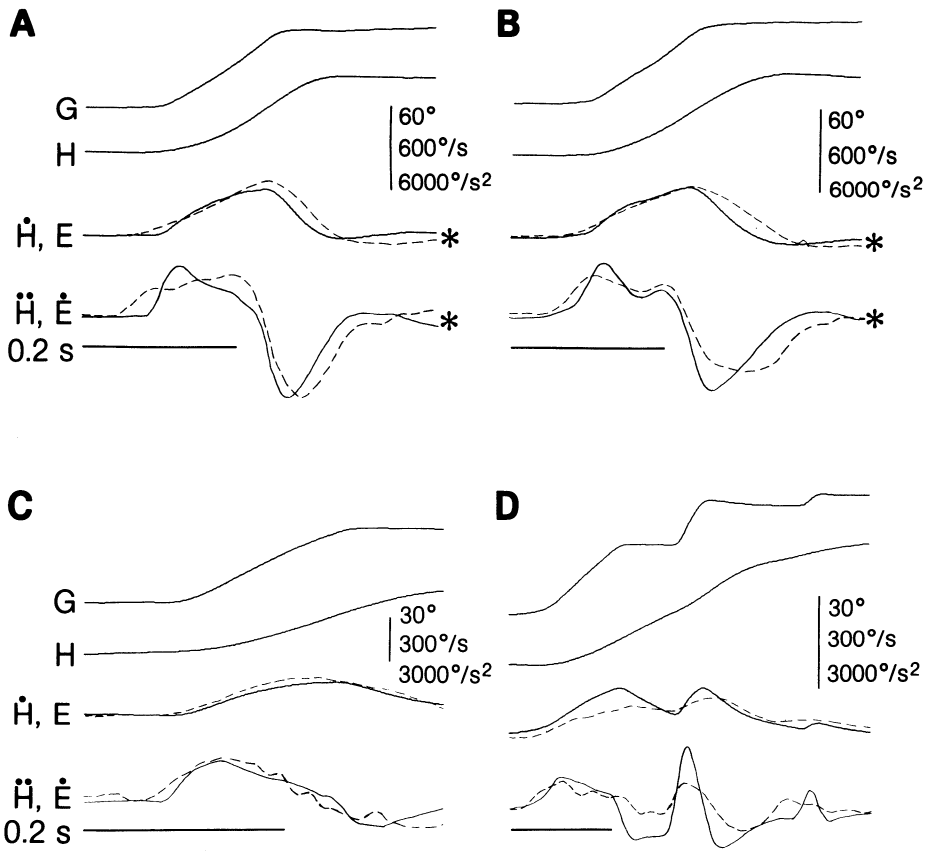

FIG. 8. Superimposition of eye- and head-movement–related traces to show the relationship between eye velocity and head acceleration. Symbols are as in Fig. 2. Eye-related traces are solid, and head-related traces are dashed. *A* and *B*: large-amplitude, visually triggered gaze shifts. In traces marked by asterisks the gain of the eye has been doubled to match that of the head. Therefore the calibration bar for eye-related traces is equal to 30 and 300°/s. *C*: predictively triggered gaze shift. *D*: double-step predictive gaze shift.

3, *E* and *F*. Additional examples are shown in Fig. 8, where the E and $\dot{H}$, and $\dot{E}$ and $\ddot{H}$, traces are superimposed for four different gaze shifts. Bearing in mind that noisy acceleration traces are inherent to the process of doubly differentiating position records, there appears a remarkable correspondence between the traces in each case over most of the duration of the head movement. Particularly noteworthy is the tight correlation between the occurrence and magnitude of peaks and valleys in the superimposed traces. Divergences between $\dot{H}$ and E appeared most often during the initial stages of head motion when gaze was stable in space and the eye compensated for head motion.

The coupling between the magnitudes of $\dot{H}$ and E throughout the gaze shift can be scrutinized more closely by the use of phase plane plots. To introduce these Fig. 9*A* shows $\ddot{H}$ versus $\dot{H}$ for ten large-amplitude gaze shifts similar to and including those of Fig. 8, *A* and *B*. The head movement begins at the origin with $\dot{H} = \ddot{H} = 0$, and the movement proceeds clockwise along the oval created by the superimposed data points. The relationship that oc-

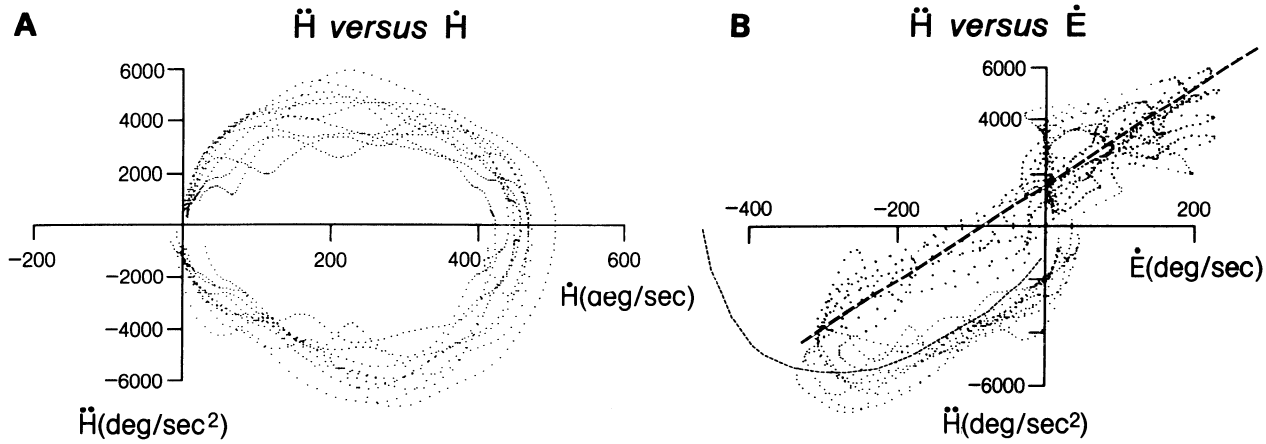

FIG. 9. Superimposition of phase plane plots from 10 large-amplitude gaze shifts such as those shown in Fig. 8, *A* and *B*. *A*: plot of head acceleration (ordinate) versus head velocity (abscissa). *B*: plot of head acceleration (ordinate) versus eye velocity (abscissa) for the same 10 trials. Dashed line shows mirror image of the average curve through points in the 2nd quadrant of the $\ddot{H}$-vs.-$\dot{H}$ curve (when gaze is steady and $\dot{E} = -\dot{H}$). Straight line through data emphasizes proposal that $\ddot{H}$ is proportional to $\dot{E}$ throughout gaze shift.

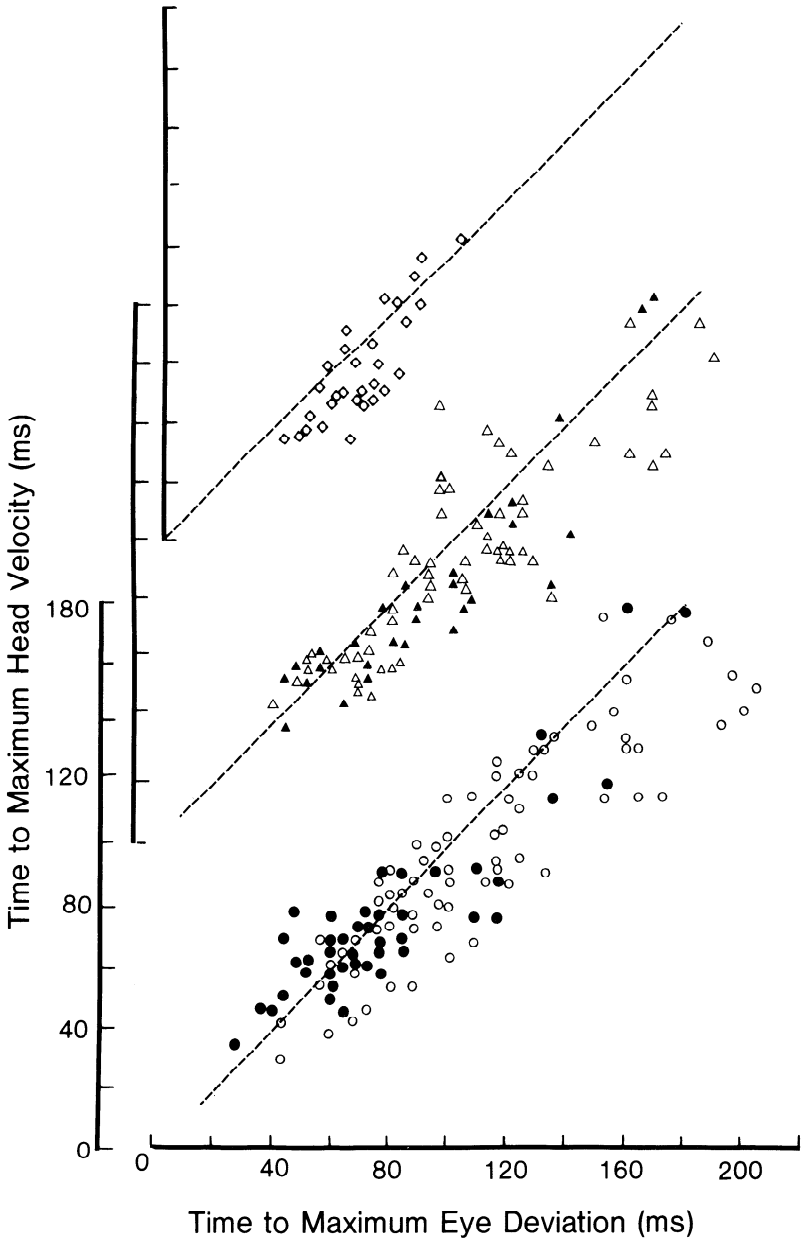

FIG. 10. Further evidence for similar eye-position and head-velocity traces is shown for 3 cats by equal times between onset of eye saccade (or gaze) and occurrence of maximum head-velocity and saccadic eye-movement deviation. Dashed line at 45° has a slope of 1. Open and closed symbols: visible- and predictive-target conditions, respectively. Circles, *cat H*; triangles, *cat Q*; diamonds, *cat S*.

curred between $\ddot{H}$ and $\dot{E}$ for these same gaze shifts is shown in Fig. 9*B*. Each of the superimposed trajectories begins just at the start of the saccadic eye movement when $\dot{E} = 0$ but where, as we saw previously (e.g., Fig. 7), $\ddot{H}$ has in some cases already attained a small positive value. Thereafter, $\ddot{H}$ and $\dot{E}$ increase (up and to the right in the first quadrant) and decrease together. The concurrent behavior of these two quantities is underlined by the fact that nearly all points lie in quadrants 1 and 3. $\ddot{H}$ and $\dot{E}$ are simultaneously either both positive (i.e., during the saccade) or both negative (i.e., during gaze stabilization). Indeed, as shown by the straight dashed line, the average relationship between $\ddot{H}$ and $\dot{E}$ is essentially linear throughout the gaze shift. Once gaze is stable in space, the eye compensates for continuing head motion. Hence $\dot{E} = -\ddot{H}$, and the data points in quadrant 3 break off into a new trajectory given by the lightly dotted line that is the mirror image of the points ($\ddot{H}$ versus $\dot{H}$) in quadrant 4 of Fig. 9*A*.

A convenient measure of the similarity between the shapes of the $\ddot{H}$ and $\dot{E}$ traces (and $\dot{H}$ and E traces) is to plot the time of occurrence of maximum $\dot{H}$ and maximum eye deviation. This is shown in Fig. 10 for three cats. Note that the points fall close to the dashed lines (slope = 1), thereby supporting the proposed tight synchrony between head and eye motion.

DISCUSSION

Movement trajectories depend on experimental paradigm

DEPENDENCE ON NEURAL ORIGIN OF SIGNALS THAT TRIGGER ORIENTING RESPONSES. The relationships linking maximum velocity, amplitude, and duration—the main sequence plots—have been described in the head-fixed cat (Blakemore and Donaghy 1980; Collewijn 1977; Crommelinck and Roucoux 1976; Evinger and Fuchs 1978; Guit-

ton et al. 1984; Guitton and Mandl 1980; Stryker and Blakemore 1972). Apart from the study by Crommelinck and Roucoux of how alertness affects maximum velocity, there has been no other report for cat of the influence of behavioral context on movement trajectories save Guitton et al. (1984), who considered this in relation to head motion.

An important feature of the observations presented in this paper is that the time course of each of the eye, head, and therefore gaze trajectories depended on the motor set or behavioral context underlying the orienting response: visually guided eye, head, and consequently gaze movements were faster than those made in the predictive-target mode whose command signals require more cognitive processing. Analogous observations made in human and monkey have demonstrated different main-sequence relationships for saccadic eye movements, depending on whether the movements were directed toward either a visible, or remembered, or predicted target or spontaneously made in the dark (Becker and Fuchs 1969; Bon and Lucchetti 1988; Hikosaka and Wurtz 1985b; Sharpe et al. 1975; Smit and Van Gisbergen 1989, Smit et al. 1987). In these studies saccades made to remembered and predicted targets were slower and had differently shaped velocity profiles than visually triggered saccades of comparable amplitude.

Such observations resemble those obtained in our barrier paradigm. In the remembered-target condition of Hikosaka and Wurtz (1985b) the trigger to orient was the extinction of the central fixation point, and the movement was made in the dark to a remembered location. In the predicted-target condition of the barrier paradigm, the trigger to orient was the disappearance of the food target from one side of the barrier. The entire room was dimly lit, so that both edges of the barrier and the laboratory surroundings were visible. Through previous training, the animal knew that disappearance of the target from one side of the barrier meant future reappearance on the other side. The animal had learned to assign significance to a specific location in its visual surrounds that depended on the width and orientation of the barrier and initial position of the food target. Similar to the reports of others cited above, the more cognitive content of the predictive-target condition in the barrier paradigm was associated with, for a given amplitude of gaze movement, lower maximum velocities of the eye, head, and therefore gaze. Furthermore, there were remarkable differences between the shapes of the gaze-velocity profiles in the visible- and predicted-target conditions with the latter exhibiting blunt or rounded peaks and irregular shapes whereas the former had sharply peaked bell-like shapes.

Such observations imply that gaze shifts may have different neural drives depending on whether the orienting movement is triggered by sensory or cognitive events. Indeed, evidence has accumulated recently suggesting that saccades generated in the head-fixed condition under direct sensory guidance are controlled by neural pathways that are different from those required to drive saccades in the absence of direct sensory inputs. For example, it has been shown that the descending pathways linking the FEF, caudate nucleus, substantia nigra, and SC play an important role in organizing cognitively generated saccades (Bruce and Goldberg 1985; Deng et al. 1986; Guitton et al. 1985; Hikosaka and Sakamoto 1986; Hikosaka et al. 1989a–c; Hikosaka and Wurtz 1983a–d, 1985a,b; Segraves and Goldberg 1987). Visually guided saccades, on the other hand, may also be driven via the SC, but the higher level command signals may differ in their origin (Keating and Gooley 1988; Pierrot-Deseilligny et al. 1987) from those used in the cognitive condition.

Combined effects of prediction and vision: modified trajectories and the minimum delay for vision to affect a movement

Whenever there was a sequential presentation of predictive and visual cues, short-latency visuomotor mechanisms affected both timing and shape of the eye- and head-movement trajectories. In our experiments the two cues were: *1*) food target disappearance from one side of the barrier that indicated to the experienced animal that the food would reappear on the other side at a specific location and *2*) food reappearance at that location.

Gaze shifts that started ~50–60 ms or more after target reappearance were similar (e.g., high-maximum velocities) to those triggered by visual stimuli in the absence of prediction with the exception that these latter gaze shifts had a latency of 100–200 ms. Therefore visual information acquired before a gaze shift began could influence the trajectories of eye and head movements (which predictive cues already had begun organizing) with the surprisingly short latency of ~50 ms. This was corroborated by the observation that midflight increases in the velocity of gaze shifts, observed after either reappearance of the food target or onset of a LED just before initiation of the gaze movement, also occurred 50–60 ms after the visual event. We have shown that these reaccelerations in gaze trajectories are, at least in part, due to visually evoked bursts in TRNs (Munoz and Guitton unpublished observations).

Extremely short-latency saccades are thought to require the SC (Schiller et al. 1987). The 50-ms latency by which visual signals influenced eye motion represents the approximate minimum theoretical delay between the onset of a visual stimulus and activation of extraocular muscle fibers. It could be made up of the afferent delay of ~40 ms required for visual information to reach TRNs and TRSNs via the direct retinotectal route (Munoz 1988; Munoz and Guitton unpublished observations). Added to this is an efferent motor delay of ~10 ms between TRN or TRSN burst discharges and the eye-movement reacceleration (Munoz and Guitton 1989, unpublished observations). Recall that a modification in the head-movement trajectory was delayed a further 20 ms, due probably to longer lags in the head plant (Zangemeister et al. 1981). In a subsequent paper (Munoz and Guitton unpublished observations) we will describe in detail the link between accelerations in the eye and head trajectories and burst discharges in the collicular efferent pathways.

The minimum delay with which a visual stimulus can trigger a saccade occurs for *express saccades* (Boch and Fischer 1986; Fischer and Boch 1983; Fischer and Ramsperger 1984; Schiller et al. 1987) and is about 70 ms in

monkey (Fischer and Boch 1983) and 100 ms in human (Fischer and Ramsperger 1984). These short latencies are thought to be due to the elimination of signals controlling attentive fixation. Interestingly, the on-line modifications in gaze trajectories described in the present results occurred at 50 ms—considerably <70 ms. The shorter latency may have resulted from the fact that movements were initiated by predictive signals and later influenced by visual signals. Because the movement had already begun, the appropriate motor and premotor neurons were in a depolarized state when the visual signal was added to the saccade signal, thereby further reducing the latency. An analogous observation is that electrical stimulation within the reticular formation shortens the latency of visually triggered saccades (Sparks et al. 1987).

Covariance of eye and head movement

The results described in this paper show in cat a very tight coupling between the eye and head movements that compose a head-free gaze shift. The following sections review results that suggest common driver signals to the eye and head motor systems.

COVARIANCE OF EYE AND HEAD VELOCITIES. Our recent hypothesis describing the control of gaze during coordinated eye-head–orienting movements postulated that saccade amplitude was dependent on the head's contribution to the gaze shift (Guitton et al. 1984; Guitton and Volle 1987). For a given amplitude gaze shift, saccade size was reduced when faster head-movements were generated. In the present experiments we found no difference in saccade amplitude when comparing gaze shifts of equal amplitude directed toward either the predicted or visible targets, although head velocities were faster in the latter condition. The eye, however, also moved faster in the visible-target mode. Indeed, the relative increase in eye velocity equalled that of the head such that the relative contributions of the eye and head to the overall gaze displacement remained constant. These observations do not contradict the earlier model (Guitton et al. 1984; Guitton and Volle 1987); rather, they complement it. Taken together the results suggest two characteristics for a hypothetical series of gaze shifts of the same amplitude but of increasing maximum velocity: first, both eye and head velocities increase together such that the contribution of the eye and head to the overall gaze displacement remains constant. Then, maximum eye velocity saturates but maximum head velocity continues to increase. It is in this latter situation that eye amplitude is inversely related to head velocity.

COVARIANCE OF EYE AND HEAD LATENCIES. Previous studies have shown that the onset of head motion precedes that of the eye in conditions where the subject can predict target onset (Bizzi et al. 1972; Zangemeister and Stark 1982a). We found that this was also the case not only for predictive gaze shifts generated by the cats in the barrier paradigm (Table 1) but also when the animals oriented to a visual target without a predictive cue. However, in most cases the early head motion was slow and contributed little to gaze displacement because its effect was nulled by compensatory eye rotation. The meaningful head movement usually began with a rapid change in head velocity that started shortly after (~20 ms) the onset of saccadic eye motion. Strong and common acceleration signals to the eyes and head also were evident in the movements whose trajectories were modified in midflight. In that condition the time difference between the onsets of eye and head reaccelerations was also ~20 ms.

In monkey (Bizzi et al. 1972, 1971) and human (Zangemeister and Stark 1982a) it has been demonstrated that bursts of neck-muscle EMG typically precede onset of head movement by ~40 ms. By comparison, eye movements are initiated ~8 ms after onset of bursts in extraocular-muscle motoneurons (Delgado-Garcia et al. 1986; Fuchs and Luschei 1970; Henn and Cohen 1973; Robinson 1970; Robinson and Keller 1972). From Table 1 we have seen that sharp head acceleration followed the onset of eye motion by between 20 and 40 ms, a value of 30 ms corresponding approximately to synchronous activation of eye and neck motoneurons.

A COMMON BURST GENERATOR FOR THE HEAD AND EYES. Saccadic eye movements are thought to be generated by a high-frequency burst discharge (the "pulse") followed by lower frequency tonic activity (the "step") responsible for holding the eye in its new position (see Fuchs et al. 1985, for review). The main thesis of this paper is that in cat the same pulse signal also contributes to driving the head. Brain stem neurons called "excitatory burst neurons" (EBNs) are believed to carry the saccade-pulse signal to the extraocular motoneurons. Although these neurons have many collaterals there is no evidence, at least in monkey, that they project to the spinal cord (Strassman et al. 1986). No analogous study involving combined anatomic and physiological identification of EBNs has yet been performed in cat. It is possible that there is a species difference with regard to a spinal projection, given a possibly tighter coupling between eye and head motion in cat compared with monkey. This could be due to the cat's limited OMR.

However, there is considerable recent evidence that the burst generator is a distributed entity in which vestibular, collicular, and reticular signals participate. For example, second-order type I vestibular neurons in cat show small bursts for contralateral saccades and project to the spinal cord (Berthoz et al. 1981; Graf and Ezure 1986; Ishizuka et al. 1980; Isu and Yokota 1983; McCrea et al. 1980, 1981, 1986; Yoshida et al. 1981). Premotor burst-tonic cells also exist in monkey vestibular nuclei (VN) (Tomlinson and Robinson 1984). RSNs in the head-fixed cat show bursts preceding both saccades and phasic components of ipsilateral neck EMG activity (Grantyn and Berthoz 1987; Grantyn et al. 1987, 1988; Vidal et al. 1983). Also, in the head-fixed cat, TRSNs (Grantyn and Grantyn 1982) burst just before saccades and phasic activity in neck muscles (Grantyn and Berthoz 1985). In the head-free cat, TRSN bursts are followed 10–15 ms later by an acceleration of the eye and 30–35 ms later by an acceleration of the head (Munoz 1988; Munoz and Guitton 1989, unpublished observations). Indeed we have proposed that the SC lies in a gaze feedback loop that drives both eye and head. In the next section we present a model of a gaze-control system in which the oculomotor burst generator also contributes a drive to the head plant.

Model of gaze-control and eye-head coupling

No comprehensive model of gaze control yet exists. Many models have assumed a head-movement trajectory rather than deriving it with the use of target error as the input (Guitton et al. 1984; Laurutis and Robinson 1986; Pélisson et al. 1988; Tomlinson 1990). Other models have been essentially conceptual schemata whose function and parameters have not been adequately explored (Guitton 1988; Guitton and Volle 1987). The object of this section is to present a model of gaze control that predicts both eye and head and therefore gaze trajectories and brings together in one unified framework the observations presented in this paper as well as many observations currently available in the literature.

In the usual approach to modeling the saccadic system in the head-fixed animal—the so-called local feedback model (Robinson 1975)—the burst generator is driven by a motor error signal obtained by subtracting actual eye position from desired eye position. As pointed out by Scudder (1988) the local feedback model requires a signal coding target-re-head as its input whereas the SC and FEF, usually regarded as inputs to the burst generator, specify the angle and direction the eye must turn to reach the target (eye motor error). To account for this discrepancy, Scudder proposed a revised version of the local feedback model that could accept an eye-motor–error signal.

An extension of the local feedback model to the head-free condition has been proposed: namely that brain stem eye and head motor circuits are driven by a gaze-motor–error signal obtained by subtracting actual gaze position from desired gaze position (Guitton 1988; Guitton et al. 1984; Guitton and Volle 1987; Laurutis and Robinson 1986; Pélisson and Prablanc 1986, 1987; Pélisson et al. 1988; Roucoux et al. 1980). However, these gaze-control models, just like the local feedback model, have some difficulties incorporating signals found in the brain stem. For example, in the model of Guitton and Volle (1987) there is a requirement for neurons coding target-position-re-space (or body), target-position-re-head, and desired eye-position-re-head, and such cells have not yet been found. There is also strong evidence that, at least in cat, the SC provides a gaze-motor–error signal and also controls simultaneously the eye and head motor circuits to drive gaze in a specific direction and through the required angle (Munoz and Guitton, 1989a,b; unpublished observations; Munoz 1988). Thus as in the local feedback model, it is of interest to seek alternative models of gaze control that operate with known signals.

The schematic in Fig. 11 presents an alternative approach to modeling the gaze-control system. It is an extension of the concepts contained in the bilateral model of the VOR originally proposed by Galiana and Outerbridge (1984), here collapsed into its one-sided form. There are fundamental differences between the model of Fig. 11 and those based on the classic local feedback model (Robinson 1975). The first is how the ocular motoneural signal is created. In the Robinson model, the "inverse eye plant" approach is used; premotor circuits compensate for plant dynamics, and motoneurons are driven by the sum of two pathways respectively coding eye velocity and its integral, eye position. In the Galiana approach used here, the moto-

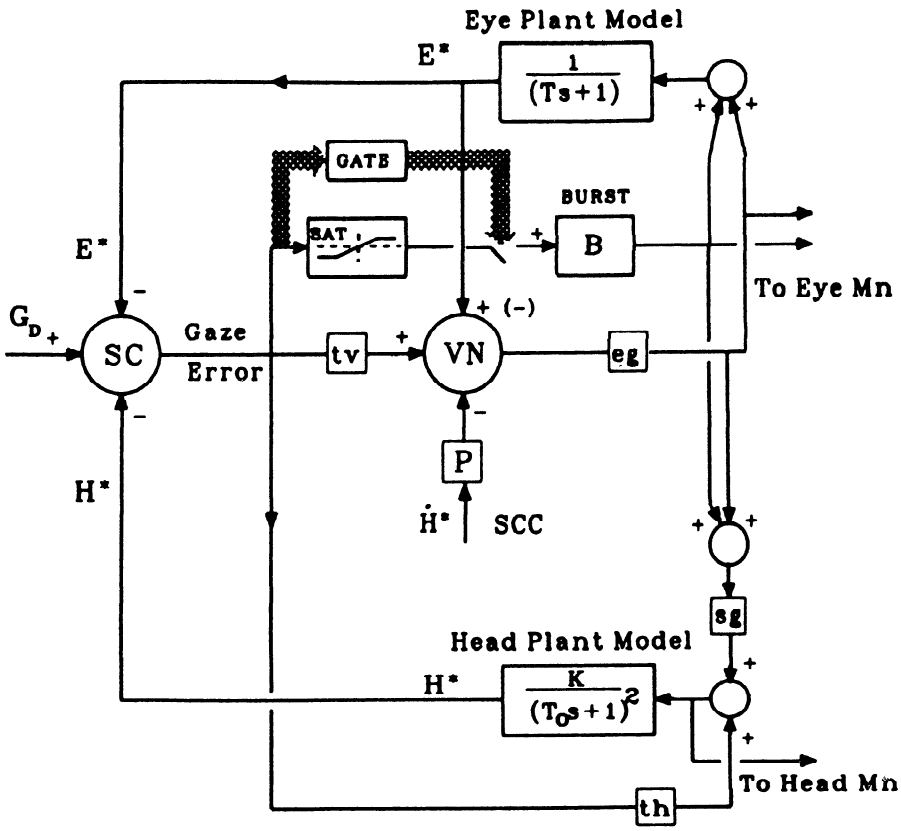

FIG. 11. Schematic model of eye-head coordination during head-free gaze shifts in the horizontal plane. Common driver signal to the eye (*top* half) and head (*bottom* half) motor systems is gaze error obtained by subtracting the sum of current eye (E^*) and head (H^*) positions from desired gaze position (G_D). Parameters used in simulations are presented in the APPENDIX. E^* and H^* are efference copies of eye-re-head and head-re-body, respectively, generated by internal models of eye and head plants, respectively. $\dot{H}^*$ is the estimate of head velocity provided by canals afferents. An important feature of the model is that the head motor system receives a copy of all ocular premotor signals, most notably the burster (B) output. Note that the sign of eye-plant-model input to VN changes between slow-phase (positive) and saccade (negative) modes (see text for more details). SC, superior colliculus; SCC, semicircular canals; VN, vestibular nuclei; B, burst generator; Gate, enables burst generator; SAT, saturation; Mn, motoneuron; *tv*, *th*, *eg*, *sg*, *K*, and *P*, gains; T_0 and T, time constants.

neurons are driven via feedback circuits through models of the eye and head plants. The two approaches to modeling are compared in the APPENDIX where simple calculations show their mathematical equivalence. No one knows for sure yet how the brain does it. The advantages of our approach are considered in subsequent paragraphs. A second difference is that the present model assumes that the SC lies within the gaze feedback loop. Although this is a controversial issue, there is mounting evidence to support this proposition (Munoz 1988; Munoz and Guitton 1989a,b, and unpublished observations; Waitzman et al. 1988), and its implementation avoids the widely assumed, though uncomfortable, alternative exemplified in the Scudder (1988) approach: that the SC—functioning open loop—knows a priori how many spikes it should send to the brain stem to drive a given amplitude gaze shift.

In Fig. 11 we have refrained from identifying many of the black boxes as specific neural structures, because the prime purpose here is to show that our control-system arrangement works. However, we believe that the neural ingredients exist to provide such a structure, and this is discussed below. We do, however, identify two major summing junctions as being the VN and SC. This is primarily because there is a need to provide a semicircular-canal input to generate compensatory eye movements; and, as stated above, some observations suggest TRSNs code instantaneous gaze error.

On the *left* of Fig. 11, desired gaze position (G_D or target-position-re-body) is compared with actual gaze position via efference copies of eye-re-head (E^*) and head-re-body (H^*) to produce an estimate of gaze error. This signal is assumed to project to head and various ocular premotor centers including a burst generator and VN. Note that each motor system to be controlled has an internal representation of its dynamics (eye and head models) that lie in the feedback loops including both the SC and VN summation points. In addition, afferent signals from the semicircular canals project via VN to the eye- and head-plant models.

As in the previously published bilateral model of the VOR (Galiana and Outerbridge 1984), the action of reticular inhibitory burst circuits on premotor networks is presumed to eliminate certain pathways and unmask others thereby leading to different dynamic properties of the oculomotor circuitry in the saccade and slow-phase modes. This important mechanism is expressed in Fig. 11 as a *sign change* of the efference copy (E^*) projection on VN: positive during slow-phase segments when gaze is stable in space and negative during the rapid gaze shifts. An automatic strategy to perform this structural change in vestibular nystagmus is described elsewhere (Galiana 1990).

Note that the SC and VN summation points represent the difference between left and right sides of the brain, and, hence, because of axons crossing the midline they drive the eye and head (and their models) through a plus sign (right-going motion is positive). During a saccade to the right for example, right excitatory burst circuits and left VN cells (such as burst-tonic neurons) drive both the eye and head toward the right. Our parameter settings are such that the relative importance of the SC burst-generator pathway on saccade dynamics is more important than that of VN (see APPENDIX) during small (<20°) gaze shifts. Because of nonlinearities the relative importance of these pathways can vary with gaze amplitude and initial eye position in the head.

OCULOMOTOR SYSTEM. The *top* one-half of Fig. 11 is concerned with how the oculomotor system is organized and has been considered at length elsewhere (Fuchs et al. 1985; Galiana and Outerbridge 1984; Munoz and Guitton 1989a; Robinson 1985). An internal model of the eye plant (first-order viscoelastic model, see APPENDIX) provides an efference copy of eye position continuously updated by collaterals from ocular premotor elements or motoneurons. During compensation for head movements, gaze error can interact with the canal signals to produce enhanced or suppressed VOR responses as required to facilitate target acquisition (Guitton 1988). In the schematic, a gate [e.g., inhibitory omnipause neurons (OPNs) in the reticular formation] releases the burst generator when gaze error from a selected target exceeds a threshold (Munoz 1988; Munoz and Guitton 1989a, unpublished observations).

During saccades gaze error is passed on to the burst generator via a saturation (in, say, long-lead bursters). This saturation limits not only eye velocity during a saccade but also, during a head-free gaze shift, imposes a neural rather than a mechanical limit to maximum eye deviations in the orbit (Guitton et al. 1984; Guitton and Volle 1987). The latter mechanism is particularly evident during large gaze shifts in which the eye will be driven to a fixed position in the orbit while the head continues to reduce gaze error. This is compatible with observed gaze shifts not only when the eye and head are initially aligned but also when the two mobile segments are not aligned at the beginning of the movement (Volle 1988). An efference copy of eye position (E^*) is used to update both gaze error and the premotor firing rates of VN cells. In a manner analoguous to the classic local feedback model (Robinson 1975), the pulse generators are driven until gaze error is within some threshold of zero.

The contribution of primary vestibular signals (canals) during saccades is not clear at this stage. It has been found that ocular saccade velocity is uninfluenced by the head-velocity signal for large gaze shifts (Guitton and Volle 1987; Laurutis and Robinson 1986; Pélisson et al. 1988; Roucoux et al. 1980; Tomlinson and Bahra 1986b). This could be due to a saturation of the canal signal during the associated large head movements, or it could simply result from the fact that the ocular motor signals are already saturated under these conditions. Because Guitton and Volle (1987) found in human no VOR during large-amplitude gaze shifts having intentionally slow head velocities, we tend toward the second argument. The simulations presented below simply assume that the canal signal is centrally disabled during the saccades; yet, because the eye and head partially share premotor signals, one would still find a relationship between eye and head velocity (a pseudo-VOR) during small gaze saccades.

HEAD MOTOR SYSTEM. The *bottom* one-half of Fig. 11 concerns the head-motor system. Here inertia plays an important part so that the head-plant model is approximated

by a critically damped second-order system (see APPENDIX). This simplification is justified on the basis of our main objective: namely, to suggest some gaze-control strategies and duplicate the experimental observations in this paper. Though the eye- and head-control systems in the schematic are depicted separately, they may in fact rely on intermingled circuits in the brain stem (see below). An important new concept is that the head plant is driven not only by gaze error but also by the same signals sent to the eye motoneurons through collateralization (Grantyn and Berthoz 1987; Grantyn and Grantyn 1982; Grantyn et al. 1987, 1988). This additional pathway easily accounts for observations in this paper, namely, the tight eye-head coupling perhaps best seen during head-free gaze shifts when ocular saccades are associated with accelerations of the head. In addition, as simulations will illustrate, it provides a basis for the eye-position dependency seen in the EMG signal of the head-fixed cat (Vidal et al. 1982), monkey (Lestienne et al. 1984), and human (André-Deshays et al. 1988).

Note particularly, in contrast to the previous models of Guitton and collaborators (Guitton et al. 1984; Guitton and Volle 1987), that there is no need to reconstruct a dedicated error for the head (i.e., head-re-target-in-space) in this shared gaze-control model. It is suggested here that a common gaze error signal is used to drive all mobile segments; it is updated by the use of efference copies of peripheral responses as extracted from internal plant models. The implication here is that only ongoing gaze motor error or premotor signals would be observed downstream of SC; a reconstructed estimate of target in space would never be needed.

Our modeling approach is speculative in its component arrangements but is compatible with neurophysiology. For example, neural motor activity coding ongoing (or dynamic) gaze error has been located in the SC in the head-free cat (Munoz 1988; Munoz and Guitton 1989b) and in the head-fixed monkey (Waitzman et al. 1988); tonic cells with activity modulated by eye position in the head (E^*) have been found in the prepositus hypoglossi (PH) (Lopez-Barneo et al. 1982), VN (McCrea et al. 1980), and pontine reticular formation (Luschei and Fuchs 1972); some tonic-vestibular cells in the VN projecting to abducens are also known to send collaterals to the spinal cord and neck motoneurons, at least in cat (McCrea et al. 1980; Uchino and Hirai 1984).

All of these neural-response data of the VN-PH have been obtained under head-fixed conditions where gaze shifts are achieved solely with eye movements. Thus observations to date cannot say whether an efference copy of

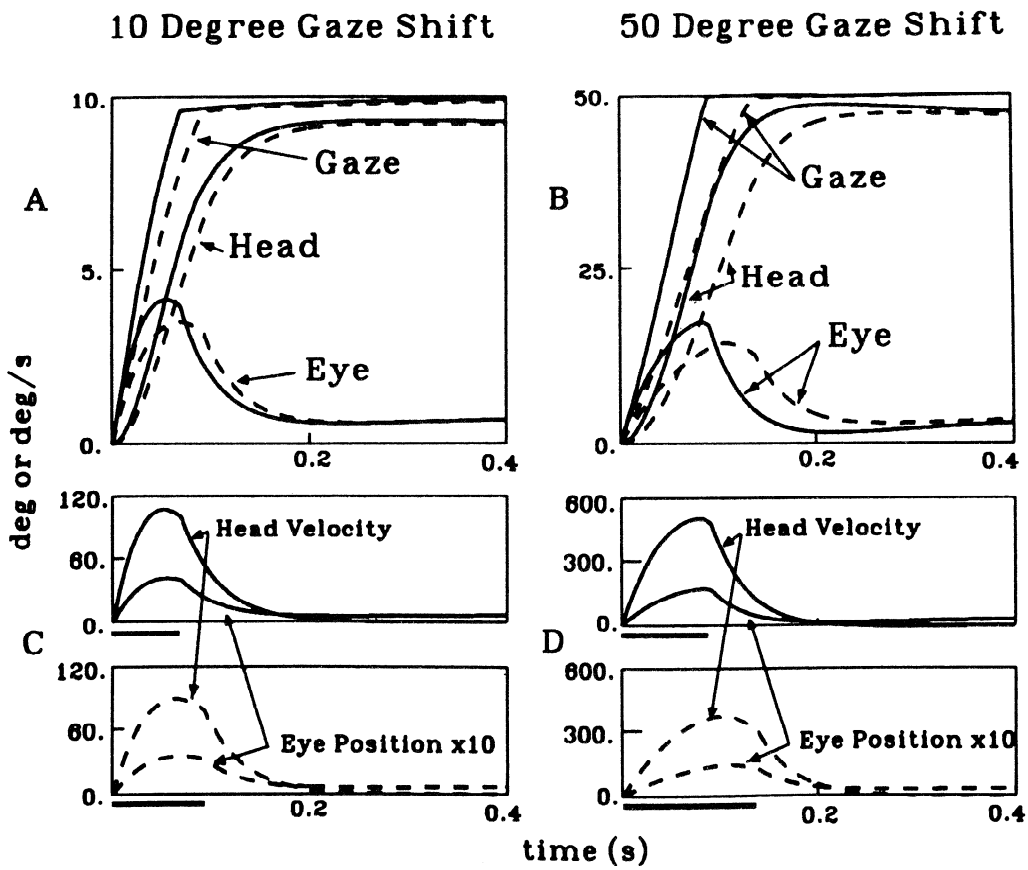

FIG. 12. *A* and *B*: simulation examples of small (10°) and large (50°) gaze shifts with the use of the model in Fig. 11 together with parameter sets defined in the APPENDIX. Solid curves represent rapid gaze shifts as presented in this paper for the case of orienting movements to visual targets; dashed curves represent slower gaze shifts, made to predicted targets, obtained by simply decreasing by identical fractions the gain between the SC gaze-error signal and its targets downstream. Note the similarity with cat data presented in Fig. 3, *E* and *F*. *C* and *D*: similarity between head-velocity and eye-position traces for fast (——) and slow (– – –) gaze shifts.

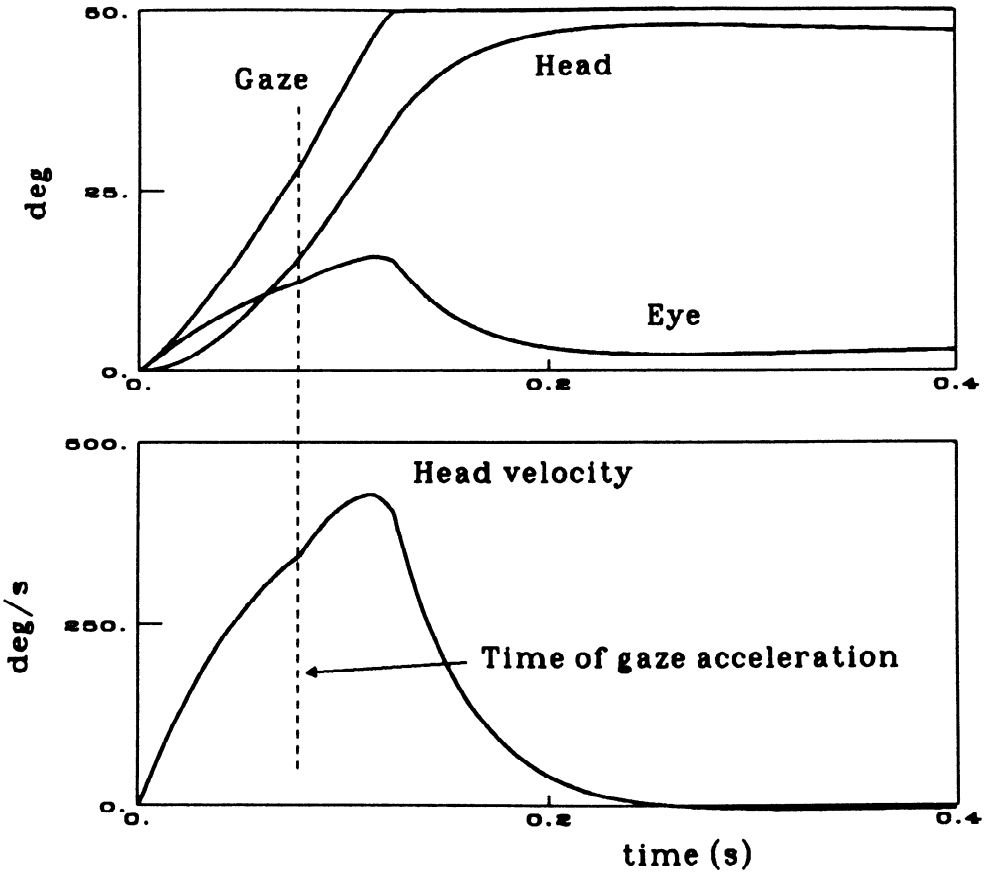

FIG. 13. Simulation example where the gaze trajectory was accelerated in midsaccade; that is, sensitivity to gaze error began with the slow parameter set of Fig. 12 and then was suddenly increased at a point 80 ms after the beginning of the gaze shift to the fast parameter set. Note that both eye and head show a synchronized increase in velocity and that the head-velocity profile closely matches that of eye position. Compare with real data in Fig. 6.

head position may also be present in these sites. An alternative during natural gaze shifts is that cells in the VN-PH complex now provide an efference copy of gaze in space ($E^* + H^*$).

The TRS pathway appears to provide one of the common motor drives to the eye and head. Indeed, these tectal efferent neurons provide the brainstem with a gaze-position error signal that is coded spatially by the distribution of neural activity on the collicular motor map (Munoz 1988; Munoz and Guitton 1985, 1989a, and unpublished observations). The intensity of the TRSN discharge appears to modulate the temporal characteristics (i.e., latency, acceleration, velocity) of the eye and head trajectories (Munoz 1988; Munoz and Guitton 1986, 1989a, and unpublished observations). Furthermore, TRSNs appear to lie in a feedback loop because the active site in the SC changes with decreasing gaze error (Munoz and Guitton 1989b, unpublished observations).

Some of the major innovations in this schematic include the following. *1*) The function of mathematical integration requires the existence of the positive feedback loop and consequently is a distributed property of the network (Galiana and Outerbridge 1984). Integration is not restricted to a single anatomic site; for example, the time constant of the eye-plant model is too short. *2*) The SC lies within a gaze feedback loop, and perforce SC output neurons code ongoing gaze error. *3*) The head and eye controls are placed inside a single gaze-error–control system, which can affect responses during both saccadic and vestibular compensatory segments. *4*) The premotor signals in the VN-PH complex may in fact be gaze related and would be used to drive simultaneously both the eye and head plants (though perhaps with a different weighting dependent on response strategy). Because VN also lies in a feedback loop, the activity of VN cells that project to the contralateral abducens nucleus will also show a burstlike profile during contralateral saccades, though normally of lesser intensity than that seen on true reticular burst cells. In addition, all burst profiles during saccades will be modulated by gaze error, or equivalently, gaze velocity. *5*) There is no need to reconstruct a signal of head-position-re-target.

SIMULATION EXAMPLES. To gain some insight into the operation of these proposed mechanisms, we have performed computer simulations of the schematic in Fig. 11 with the use of the parameter set defined in the APPENDIX, which reproduced observed behavior in cat as described in this paper.

Gaze shifts to visual targets had shorter durations and larger eye and head velocities than comparable amplitude and direction movements to predicted targets. These behavioral observations are associated with changes in the

peak firing rates of TRNs and TRSNs at a given location in the SC (Munoz 1988; Munoz and Guitton 1986, 1989a, and unpublished observations). Because the model in Fig. 11 uses feedback through the colliculus, it is possible to generate faster gaze shifts by increasing the gain (or sensitivity) between the TRSN gaze-error signal and its target areas, without changing the end-point of the gaze saccade. This is illustrated in Fig. 12, in which small (10°) and large (50°) gaze shifts were simulated. The faster gaze shifts were obtained by multiplying all gaze-error (i.e., TRSN) projections (*th*, *tv*, and SAT gain) by a factor of 3.

These simulations compare very well with the behavioral data. There is a higher velocity in both the eye and head contributions during faster gaze shifts: rapid gaze shifts are associated with simultaneous accelerations in the head and eye contributions, so that there is no apparent VOR-induced reduction of the eye response during faster head movements (Fig. 3). Furthermore, the saccadic eye-movement amplitude remains about equal in the slow and fast gaze shifts (Fig. 4). This is due to the activation of the saturation element (SAT) that acts to limit maximal eye deviation in the orbit. It is worth noting here that the saccade is defined as that segment of the response where gaze error is not zero and that this corresponds to a closed gate in Fig. 11 or, neurophysiologically, to the pause interval on OPNs. The period when the gate is closed is indicated by a heavy horizontal line beneath each section of Fig. 12, *C* and *D*. An interesting emergent property of the model is that the eye can turn around and move in a "compensatory" direction (a pseudo-VOR) near the end of the gaze saccade, even though OPNs are still silent and there is no canal input to VN ($P = 0$). Preliminary findings from our laboratory have revealed that OPNs do indeed pause for the duration of the gaze saccade even when the eye is moving in the compensatory direction (Paré and Guitton 1989). Note further in Fig. 12, *C* and *D*, the very close resemblance between the $\dot{H}$ and E profiles, again in agreement with experimental results (Figs. 3, *E* and *F*, and 8).

The coupling of eye and head trajectories is illustrated even more dramatically in Fig. 13 where a change in TRSN burst intensity was assumed to occur on-line, 80 ms into the gaze shift. The simulations duplicate data (Fig. 6) when a visual target suddenly appeared during a gaze shift to its predicted location. It was generated by simulating the model with the use of the slow parameter set (– – – in Fig. 12) at the beginning of the gaze shift, and then suddenly increasing, by a factor of 3, the TRSN-projection strengths (gains *tv*, *th*, and SAT) 80 ms into the saccade. This would be associated, as shown by Munoz and Guitton (1989a, unpublished observations), with a sudden increase in the bursting activity of TRSNs on the appearance of the target at the onset of a predictive movement. Note also the covariance of eye-position and head-velocity profiles, the synchrony in their peak values, and their parallel increase during faster trajectories.

APPENDIX

Comparing oculomotor models

A simple exercise can show the equivalence of the modeling approach used here to more generally accepted models (Robinson 1975) of oculomotor control. The representations in Laplace transforms on the *left* of Fig. 14 use the inverse of the eye plant to shape the motoneural drive; the approaches on the *right* rely instead on model reference feedback, so that plant inversion is not necessary.

In the case of fixation or slow-phase vestibular compensation, where it is required to provide the function of central integration, we can refer to the two *top* schemata in Fig. 14 (*A* and *B*). The synthesis of appropriate ocular motoneural signals is normally represented as the sum of two pathways, one carrying desired eye velocity, whereas the other carries the integral of eye velocity, i.e., desired eye position. These signals are denoted as $\dot{E}^*$ and E^*, respectively, in Fig. 14*A*, where the "neural integrator" (NI) is assumed to have a large time constant, T'. The equivalent overall transfer function between input and generated motoneural signal is indicated in the figure by the expression for the ratio M/I. The assumption here is that a first-order model of the eye plant is adequate and that premotor circuits must compensate for eye-plant dynamics. In the alternate approach first proposed by Galiana and Outerbridge (1984) an efference copy of eye position is obtained by driving an internal model of the eye plant with the same motor signals as the peripheral plant, as shown in Fig. 14*B*. Here the function of mathematical integration arises from the dynamics of positive feedback loops (which also include cross-midline circuits in the bilateral form), so that the NI is now a distributed property of interconnections between premotor nuclei, rather than an isolated dedicated network (compare Fig. 14, *A* and *B*). However, note that in terms of the synthesized motoneural signals, the transfer functions with respect to the input drive "I" are perfectly equivalent in the two cases.

During saccades or quick phases (Fig. 14, *C* and *D*) the classical approach now drives the plant-compensation circuit solely with the output of reticular burst cells (*B*). The bursts are modulated by an estimate of motor error, which is derived by comparing desired eye position (E_d) with an efference copy of actual eye position (E^*) through internal feedback (Robinson 1975). In the alternate approach (Fig. 14*D*) the model of the eye plant is now used in negative feedback loops that update both burst (*B*) and other premotor signals; the activity of this other premotor pathway (e.g., burst-tonic cells in the VN) may not reflect as large a burst as on the reticular burst cell, but it can nevertheless play an important role in the saccade dynamics because it contributes an additional loop to the circuits. Both types of saccadic models (Fig. 14, *C* and *D*) require the presence of the reticular burst cells to interact with OPNs and enable the transformation to the saccadic mode. Again, we find that both approaches can provide equivalent drives to the motoneuron during saccades (M/E_D). However, they have different implications in terms of neural circuitry and the expected effect of lesions on the properties of saccades and the central neural integrator.

Parameters of the gaze-control model

The model reference approach is extended in Fig. 11 to include models of both the eye and head plants during gaze control (see DISCUSSION). In the interest of clarity and for the purposes of this paper, some pathways used in the original bilateral model of the VOR have been left out. Hence, for example, the model in Fig. 11 could not generate pure vestibular quick phases without resorting to a participation of the SC. Future expansions on our simplified schema should consider VN-B interconnections and their role in the generation of vestibularly induced quick phases (Galiana 1987, unpublished observations; Guitton 1988; Guitton et al. 1984).

In Fig. 11 we have simply represented the eye plant as a first-order, low-pass filter and the head plant as a second-order critically damped system. An important advantage of using feedback through plant models is that the characteristics of eye and head

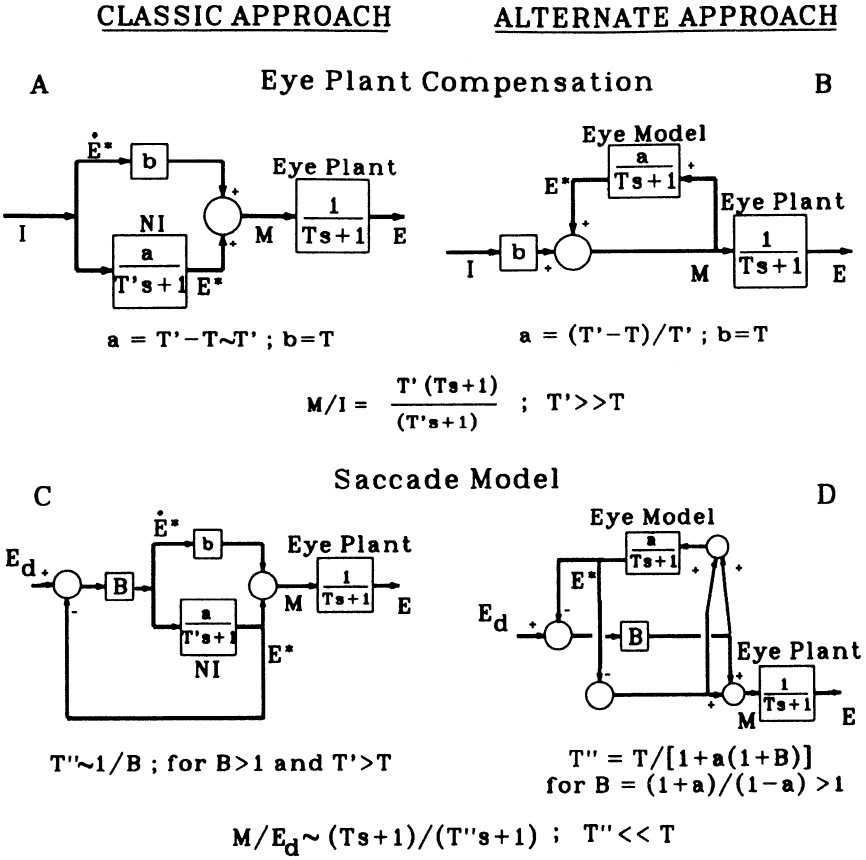

FIG. 14. Two approaches to the synthesis of ocular motoneural signals. *Left* column represents the use of parallel summed pathways to provide an inverse of eye-plant dynamics (Robinson, 1975); here the input is assumed to represent desired eye velocity ($\dot{E}^*$), which must be processed by a dedicated neural integrator (NI) to provide an efference copy of eye position (E^*); E is the actual eye position. *Right* column represents an alternative approach where the motoneural signal is shaped simply by the use of feedback through an internal model of the eye plant (Galiana and Outerbridge 1984). Slow phases or fixation signals that require a "holding" capability are represented in the top row (*A* and *B*). Saccade generation is represented in the 2nd row (*C* and *D*) where the addition of burster circuits now modifies response dynamics to generate very rapid eye movements. *C* represents Robinson's local feedback model. Transfer functions between M/I and M/E_d are shown below the *top* and *bottom* rows, respectively. Note that both approaches can provide exactly equivalent dynamics in slow or fast phases, including a term in the numerator that cancels eye-plant dynamics. See text for further details.

trajectories are relatively insensitive to the accuracy of the model used: the only condition being that the head plant be more sluggish than the eye plant. In the simulation we assume perfect models so that E^* and H^* (plotted in Figs. 12 and 13) are exactly equivalent to the real eye and head trajectories. Parameters used in the simulations are listed below, where numbers in brackets represent values used only during the saccade mode (when GATE enables the burst pathway). Similarly, because of changes in central connections between the slow phase and saccadic modes (see text), it is postulated that the sign of an excitatory pathway is reversed to inhibition during saccades (Fig. 14, and minus sign in brackets in Fig. 11). Note that to assure continuity of initial condition on the boxes as the model switches from one mode to another, it is important that separate models of slow- and quick-phase modes not be used: i.e., each plant model should appear only once in the simulation and only its inputs switched according to the mode used. Furthermore, users of commercial simulation software packages should be aware that libraries of transfer functions are not always properly implemented for switching circuits; it is generally safer to implement transfer functions oneself.

Inputs to the gaze-control model consisted of steps on G_D. Saccadic mode was triggered for gaze errors $>2°$ and terminated when the error was reduced to 0.5°. This was implemented in the GATE box that kept the switch open during slow phases (burst cells silent) and closed it during saccades. All simulations were performed at step intervals of 1 ms. The parameter set below, defining time constants and gains, corresponds to that used for the slower movements in Fig. 12, or the initial segment of Fig. 13

T = 200 ms	K = 2.9
T_0 = 300 ms	eg = 0.98, slow phase (0.5, saccade)
tv = 0.67	sg = 4.0
th = 0.67	P = 0.2, slow phase (0.0, saccade)
B = 2.0	Sat = gain of 1.0 with output amplitude saturation ± 15.0

The faster trajectories resulted from a parallel, tripling increase in the gain of all gaze-error projections, i.e., by the use of th = 2.0, tv = 2.0, and a gain of SAT = 3.0, with the same saturation level of 15. These parameter sets provided a gaze holding-time constant of 12 s in the dark; a VOR gain for passive head rotation of 1 (positive loop enhances effect of gain P), and assumed no canal influence during the saccade (P = 0 during saccades). Even if the canal signal remained significant during saccades ($P > 0$), realistic response trajectories could be achieved via suitable changes in parameters. In closing we again underline the robustness of this modelling approach: the shapes of the eye and head trajectories are generally insensitive to changes in the parameters; only the time scales are.

We are very grateful to R. M. Douglas (Dept. Ophthalmology, University of British Columbia, Vancouver, Canada), who wrote the computer software and contributed extensively to the installation and development of our computing facility. The technical and secretarial assistance of M. Feran, M. Mazza, J. Roy, S. Schiller, and J. Thibaudeau is also acknowledged.

This work was supported by the Medical Research Council of Canada and le Fonds de la Recherche en Santé du Québec. D. P. Munoz was supported by a Medical Research Council Studentship and a smaller stipend from the Montreal Neurological Institute.

Present address of D. P. Munoz: Laboratory of Sensorimotor Research, National Eye Institute, National Institutes of Health, Bldg. 10, Rm. 10C101, Bethesda, MD 20892.

Address for reprint requests: D. Guitton, Montreal Neurological Institute, 3801 University Street, Montreal, Québec H3A 2B4, Canada.

Received 31 January 1989; accepted in final form 20 March 1990.

REFERENCES

ANDRE-DESHAYS, C., BERTHOZ, A., AND REVEL, M. Eye-head coupling in humans. I. Simultaneous recording of isolated motor units in dorsal

neck muscles and horizontal eye movements. *Exp. Brain Res.* 69: 399–406, 1988.

BARNES, G. R. Vestibulo-ocular function during co-ordinated head and eye movements to acquire visual targets. *J. Physiol. Lond.* 287: 127–147, 1979.

BECKER, W. AND FUCHS, A. F. Further properties of the human saccadic system: eye movements and correction saccades with and without visual fixation points. *Vision Res.* 9: 1247–1258, 1969.

BERTHOZ, A. AND GRANTYN, A. Neuronal mechanisms underlying eye-head coordination. In: *Progress in Brain Research,* edited by H. J. Freund, U. Büttner, B. Cohen, and J. Noth. Amsterdam: Elsevier/North Holland, 1986, p. 325–343.

BERTHOZ, A., YOSHIDA, K., AND VIDAL, P. P. Horizontal eye movement signals in second order vestibular nuclei neurons in the alert cat. *Ann. NY Acad. Sci.* 374: 144–156, 1981.

BIZZI, E. Eye-head coordination. In: *Handbook of Physiology. The Nervous System.* Bethesda, MD: Am. Physiol. Soc., 1981, vol. II, p. 1321–1336.

BIZZI, E., KALIL, R. E., AND MORASSO, P. Two modes of active eye-head coordination in monkeys. *Brain Res.* 40: 45–48, 1972.

BIZZI, E., KALIL, R. E., AND TAGLIASCO, V. Eye-head coordination in monkeys: evidence for centrally patterned organization. *Science Wash. DC* 173: 452–454, 1971.

BLAKEMORE, C. AND DONAGHY, M. Co-ordination of head and eyes in the gaze changing behavior of cats. *J. Physiol. Lond.* 300: 317–335, 1980.

BOCH, R. AND FISCHER, B. Further observations on the occurrence of express-saccades in the monkey. *Exp. Brain Res.* 63: 487–494, 1986.

BON, L. AND LUCCHETTI, C. The motor programs of monkey's saccades: an attentional hypothesis. *Exp. Brain Res.* 71: 199–207, 1988.

BRUCE, C. J. AND GOLDBERG, M. E. Primate frontal eye fields. I. Single neurons discharging before saccades. *J. Neurophysiol.* 53: 603–635, 1985.

COLLEWIJN, H. Gaze in freely moving subjects. In: *Control of Gaze by Brain Stem Neurons,* edited by R. Baker and A. Berthoz. Amsterdam: Elsevier/North-Holland, 1977, p. 13–22.

CROMMELINCK, M. AND ROUCOUX, A. Characteristics of cat's eye saccades in different states of alertness. *Brain Res.* 103: 574–578, 1976.

DELGADO-GARCIA, J. M., DEL POZO, F., AND BAKER, R. Behavior of neurons in the abducens nucleus of the alert cat. I. Motoneurons. *Neuroscience* 17: 929–952, 1986.

DENG, S.-Y., GOLDBERG, M. E., SEGRAVES, M. A., UNGERLEIDER, L. G., AND MISHKIN, M. The effect of unilateral ablation of frontal eye fields on saccade performance in the monkey. In: *Adaptive Processes in the Visual and Oculomotor Systems,* edited by E. Keller and D. Zee. New York: Elsevier/North-Holland, 1986, p. 201–208.

EVINGER, C. AND FUCHS, A. F. Saccadic, smooth pursuit, and optokinetic eye movements of the trained cat. *J. Physiol. Lond.* 285: 209–229, 1978.

FISCHER, B. AND BOCH, R. Saccadic eye movements after extremely short reaction times in the monkey. *Brain Res.* 260: 21–26, 1983.

FISCHER, B. AND RAMSPERGER, E. Human express saccades: extremely short reaction times of goal directed eye movements. *Exp. Brain Res.* 57: 191–195, 1984.

FUCHS, A. F., KANEKO, C. R. S., AND SCUDDER, C. A. Brainstem control of saccadic eye movements. *Annu. Rev. Neurosci.* 8: 307–337, 1985.

FUCHS, A. F. AND LUSCHEI, E. S. Firing patterns of abducens neurons of alert monkeys in relationship to horizontal eye movement. *J. Neurophysiol.* 33: 382–392, 1970.

FULLER, J. H. Linkage of eye and head movements in the alert rabbit. *Brain Res.* 194: 219–222, 1980.

FULLER, J. H., MALDONADO, H., AND SCHLAG, J. Vestibular-oculomotor interaction in cat eye-head movements. *Brain Res.* 271: 241–250, 1983.

FUNK, C. J. AND ANDERSON, M. E. Saccadic eye movements and eye-head coordination in children. *Percept. Mot. Skills* 44: 599–610, 1977.

GALIANA, H. L. The implications of structural modulation in the vestibulo-ocular reflex. *Proc. IEEE Montech 1987 Conf. Biomed. Techn.,* p. 15–18.

GALIANA, H. L. A nystagmus strategy to linearize the vestibulo-ocular reflex. *IEEE Trans. Biomed. Eng.* In press.

GALIANA, H. L., GUITTON, D., AND MUNOZ, D. P. Modelling head-free gaze control in the cat. In: *IBRO Symposium Series, Vol. 2. Proceedings of the Head-Neck Symposium, Fontainebleau, July 16–20, 1989,* edited by A. Berthoz, P. P. Vidal, and W. Graf. Sussex, UK: Wiley, 1990.

GALIANA, H. L. AND OUTERBRIDGE, J. S. A bilateral model for central neural pathways in the vestibulo-ocular reflex. *J. Neurophysiol.* 51: 210–241, 1984.

GRAF, W. AND EZURE, K. Morphology of vertical canal related second order vestibular neurons in the cat. *Exp. Brain Res.* 63: 35–48, 1986.

GRANTYN, A. AND BERTHOZ, A. Burst activity of identified tecto-reticulo-spinal neurons in the alert cat. *Exp. Brain Res.* 57: 417–421, 1985.

GRANTYN, A. AND BERTHOZ, A. Reticulo-spinal neurons participating in the control of synergistic eye and head movements during orienting in the cat. I. Behavioral properties. *Exp. Brain Res.* 66: 339–354, 1987.

GRANTYN, A. AND GRANTYN, R. Axonal patterns and sites of termination of cat superior colliculus neurons projecting in the tecto-bulbo-spinal tract. *Exp. Brain Res.* 46: 243–256, 1982.

GRANTYN, A., HARDY, O., AND BERTHOZ, A. Activity and ponto-bulbar connections of reticulo-spinal neurons subserving visually triggered orienting eye and head movements. *Soc. Neurosci. Abstr.* 14: 959, 1988.

GRANTYN, A., ONG-MEANG JACQUES, V., AND BERTHOZ, A. Reticulospinal neurons participating in the control of synergic eye and head movements during orienting in the cat. II. Morphological properties as revealed by intra-axonal injections of horseradish peroxidase. *Exp. Brain Res.* 66: 355–377, 1987.

GRESTY, M. A. Coordination of head and eye movements to fixate continuous and intermittent targets. *Vision Res.* 14: 395–403, 1974.

GUITTON, D. On the participation of the feline "frontal eye field" in the control of eye and head movements. In: *Progress in Oculomotor Research,* edited by A. Fuchs and W. Becker. Amsterdam: Elsevier/North Holland, 1981, p. 193–201.

GUITTON, D. Eye-head coordination in gaze control. In: *Control of Head Movement,* edited by B. W. Peterson and F. J. Richmond. Oxford, UK: Oxford Univ. Press, 1988, p. 196–207.

GUITTON, D., BUCHTEL, H. A., AND DOUGLAS, R. M. Frontal lobe lesions in man cause difficulties in suppressing reflexive glances and in generating goal-directed saccades. *Exp. Brain Res.* 58: 455–472, 1985.

GUITTON, D., CROMMELINCK, M., AND ROUCOUX, A. Stimulation of the superior colliculus in the alert cat. I. Eye movements and neck EMG activity evoked when the head is restrained. *Exp. Brain Res.* 39: 63–73, 1980.

GUITTON, D., DOUGLAS, R. M., AND VOLLE, M. Eye-head coordination in cats. *J. Neurophysiol.* 52: 1030–1050, 1984.

GUITTON, D. AND MANDL, G. Frontal 'oculomotor' area in alert cat. I. Eye movements and neck muscle activity evoked by stimulation. *Brain Res.* 149: 295–312, 1978a.

GUITTON, D. AND MANDL, G. Frontal 'oculomotor' area in alert cat. II. Unit discharges associated with eye movements and neck muscle activity. *Brain Res.* 149: 313–327, 1978b.

GUITTON, D. AND MANDL, G. A comparison between saccades and quick phases of vestibular nystagmus in the cat. *Vision Res.* 20: 865–873, 1980.

GUITTON, D. AND MUNOZ, D. P. Gaze control in head-free cats: task dependent trajectories and evidence for a common motor drive to the eyes and head. *Soc. Neurosci. Abstr.* 14: 612, 1988.

GUITTON, D. AND VOLLE, M. Gaze control in humans: eye-head coordination during orienting movements to targets within and beyond the oculomotor range. *J. Neurophysiol.* 58: 427–459, 1987.

HENN, V. AND COHEN, B. Quantitative analysis of activity in eye muscle motoneurons during saccadic eye movements and positions of fixation. *J. Neurophysiol.* 36: 115–126, 1973.

HIKOSAKA, O. AND SAKAMOTO, M. Cell activity in monkey caudate nucleus preceding saccadic eye movements. *Exp. Brain Res.* 63: 659–662, 1986.

HIKOSAKA, O., SAKAMOTO, M., AND USUI, S. Functional properties of monkey caudate neurons. I. Activities related to saccadic eye movements. *J. Neurophysiol.* 61: 780–798, 1989a.

HIKOSAKA, O., SAKAMOTO, M., AND USUI, S. Functional properties of monkey caudate neurons. II. Visual and auditory responses. *J. Neurophysiol.* 61: 799–813, 1989b.

HIKOSAKA, O., SAKAMOTO, M., AND USUI, S. Functional properties of monkey caudate neurons. III. Activities related to expectation of target and reward. *J. Neurophysiol.* 61: 814–832, 1989c.

HIKOSAKA, O. AND WURTZ, R. H. Visual and oculomotor functions of monkey substantia nigra pars reticulata. I. Relation of visual and auditory responses to saccades. *J. Neurophysiol.* 49: 1230–1253, 1983a.

HIKOSAKA, O. AND WURTZ, R. H. Visual and oculomotor functions of

monkey substantia nigra pars reticulata. II. Visual responses related to fixation of gaze. *J. Neurophysiol.* 49: 1254–1267, 1983b.

HIKOSAKA, O. AND WURTZ, R. H. Visual and oculomotor functions of monkey substantia nigra pars reticula. III. Memory-contingent visual and saccade responses. *J. Neurophysiol.* 49: 1268–1284, 1983c.

HIKOSAKA, O. AND WURTZ, R. H. Visual and oculomotor functions of monkey substantia nigra pars reticulata. IV. Relation of substantia nigra to superior colliculus. *J. Neurophysiol.* 49: 1285–1301, 1983d.

HIKOSAKA, O. AND WURTZ, R. H. Modification of saccadic eye movements by GABA-related substances. I. Effect of muscimol and bicuculline in monkey superior colliculus. *J. Neurophysiol.* 53: 266–291, 1985a.

HIKOSAKA, O. AND WURTZ, R. H. Modification of saccadic eye movements by GABA-related substances. II. Effects of muscimol in monkey substantia nigra pars reticulata. *J. Neurophysiol.* 53: 292–308, 1985b.

HUERTA, M. F., KRUBITZER, L. A., AND KAAS, J. H. Frontal eye field as defined by intracortical microstimulation in squirrel monkeys, owl monkeys, and macaque monkeys. I. Subcortical connections. *J. Comp. Neurol.* 253: 415–439, 1986.

ISHIZUKA, N., MANNEN, H., SASAKI, S., AND SHIMAZU, H. Axonal branches and terminations in the cat abducens nucleus of secondary vestibular neurons in the horizontal canal system. *Neurosci. Lett.* 16: 143–148, 1980.

ISU, N. AND YOKOTA, J. Morphophysiological study on the divergent projection of axon collaterals of medial vestibular nucleus neurons in the cat. *Exp. Brain Res.* 53: 151–162, 1983.

KEATING, E. G. AND GOOLEY, S. G. Disconnection of parietal and occipital access to the saccadic oculomotor system. *Exp. Brain Res.* 70: 385–398, 1988.

LAURUTIS, V. P. AND ROBINSON, D. A. The vestibulo-ocular reflex during human saccadic eye movements. *J. Physiol. Lond.* 373: 209–233, 1986.

LEICHNETZ, G. R. The prefrontal cortico-oculomotor trajectories in the monkey. *J. Neurol. Sci.* 49: 387–396, 1981.

LESTIENNE, F., VIDAL, P. P., AND BERTHOZ, A. Gaze changing behavior in head restrained monkey. *Exp. Brain Res.* 53: 349–356, 1984.

LOPEZ-BARNEO, J., DARLOT, C., BERTHOZ, A., AND BAKER, R. Neuronal activity in prepositus nucleus correlated with eye movement in the alert cat. *J. Neurophysiol.* 47: 329–352, 1982.

LUSCHEI, E. S. AND FUCHS, A. Activity of brain stem neurons during eye movements of alert monkeys. *J. Neurophysiol.* 35: 445–461, 1972.

MCCREA, R. A., MINOR, L. B., AND GOLDBERG, J. M. Collateral projections of medial vestibulospinal tract neurons to the extraocular motor nuclei in the squirrel monkey. *Soc. Neurosci. Abstr.* 12: 457, 1986.

MCCREA, R. A., YOSHIDA, K., BERTHOZ, A., AND BAKER, R. Eye movement related activity and morphology of second order vestibular neurons terminating in the cat abducens nucleus. *Exp. Brain Res.* 40: 468–473, 1980.

MCCREA, R. A., YOSHIDA, K., EVINGER, C., AND BERTHOZ, A. The location, axonal arborization and termination sites of eye-movement-related secondary vestibular neurons demonstrated by intra-axonal HRP injection in the alert cat. In: *Progress in Oculomotor Research,* edited by A. Fuchs and W. Becker. Amsterdam: Elsevier/North Holland, 1981, p. 379–386.

MELVILL JONES, G., GUITTON, D., AND BERTHOZ, A. Changing patterns of eye-head coordination during 6h of optically reversed vision. *Exp. Brain Res.* 69: 531–544, 1988.

MORASSO, P., BIZZI, E., AND DICHGANS, J. Adjustment of saccade characteristics during head movements. *Exp. Brain Res.* 16: 492–500, 1973.

MOSCHOVAKIS, A. B. AND KARABELAS, A. B. Observations on the somadendritic morphology and axonal trajectory of intracellularly HRP-labelled efferent neurons located in the deeper layers of the superior colliculus of the cat. *J. Comp. Neurol.* 239: 279–308, 1985.

MOSCHOVAKIS, A. B., KARABELAS, A. B., AND HIGHSTEIN, S. M. Structure-function-relationships in the primate superior colliculus. I. Morphological classification of efferent neurons. *J. Neurophysiol.* 60: 232–262, 1988a.

MOSCHOVAKIS, A. B., KARABELAS, A. B., AND HIGHSTEIN, S. M. Structure-function-relationships in the primate superior colliculus. II. Morphological identity of presaccadic neurons. *J. Neurophysiol.* 60: 263–302, 1988b.

MUNOZ, D. P. *On the Role of the Tecto-Reticulo-Spinal System in Gaze Control* (PhD thesis). Montréal, Canada: McGill Univer., 1988.

MUNOZ, D. P. AND GUITTON, D. Tectospinal neurons in the cat have discharges coding gaze position error. *Brain Res.* 341: 184–188, 1985.

MUNOZ, D. P. AND GUITTON, D. Presaccadic burst discharges of tecto-reticulo-spinal neurons in the alert head-free cat. *Brain Res.* 398: 185–190, 1986.

MUNOZ, D. P. AND GUITTON, D. Fixation and orientation control by the tecto-reticulo-spinal system in the cat whose head is unrestrained. *Rev. Neurol. Paris* 145: 567–579, 1989.

MUNOZ, D. P., GUITTON, D., AND PÉLISSON, D. Gaze control in the head-free cat. II. Spatio-temporal variations in the discharge of superior colliculus output neurons. *Soc. Neurosci. Abstr.* 15: 807, 1989.

PARE, M. AND GUITTON, D. Gaze-related activity of brainstem omnipause neurons recorded in the alert head-free cat. *Soc. Neurosci. Abstr.* 15: 239, 1989.

PELISSON, D. AND PRABLANC, C. Vestibulo-ocular reflex (VOR) induced by passive head rotation and goal-directed saccadic eye movements do not simply add in man. *Brain Res.* 380: 397–400, 1986.

PELISSON, D. AND PRABLANC, C. Gaze control in man: evidence for vestibulo-ocular reflex inhibition during goal directed saccadic eye movements. In: *Eye Movements: From Physiology to Cognition,* edited by J. K. O'Regan and A. Lévy-Schoen. Amsterdam: Elsevier/North Holland, 1987, p. 237–246.

PELISSON, D., PRABLANC, C., AND URQUIZAR, C. Vestibuloocular reflex inhibition and gaze saccade control characteristics during eye-head orientation in humans. *J. Neurophysiol.* 59: 997–1013, 1988.

PIERROT-DESEILLIGNY, C., RIVAUD, S., PENET, C., AND RIGOLET, M. H. Latencies of visually guided saccades in unilateral hemispheric cerebral lesions. *Ann. Neurol.* 21: 138–148, 1987.

ROBINSON, D. A. A method of measuring eye movement using a scleral search coil in a magnetic field. *IEEE Trans. Bio-Med. Electron.* BME-10: 137–145, 1963.

ROBINSON, D. A. Oculomotor unit behavior in the monkey. *J. Neurophysiol.* 33: 393–404, 1970.

ROBINSON, D. A. Oculomotor control signals. In: *Basic Mechanisms of Ocular Motility and Their Clinical Implications,* edited by G. Lennerstrand and P. Bach-y-Rita. Oxford, UK: Pergamon, 1975, p. 337–374.

ROBINSON, D. A. Models of the mechanics of eye movements. In: *Models of Oculomotor Behavior and Control,* edited by B. L. Zuber. Boca Raton, FL: CRC, 1981, p. 21–41.

ROBINSON, D. A. AND KELLER, E. L. The behavior of eye movement motoneurons in the alert monkey. *Bibl. Ophthalmol.* 82: 7–16, 1972.

ROUCOUX, A., GUITTON, D., AND CROMMELINCK, M. Stimulation of the superior colliculus in the alert cat. II. Eye and head movements evoked when the head is unrestrained. *Exp. Brain Res.* 39: 75–85, 1980.

ROUCOUX, A., VIDAL, P. P., VERAART, C., CROMMELINCK, M., AND BERTHOZ, A. The relation of neck muscle activity to horizontal eye position in the alert cat. I. Head-fixed. In: *Physiological and Pathological Aspects of Eye Movements,* edited by A. Roucoux and M. Crommelinck. The Hague: Junk, 1982, p. 371–378.

SCHILLER, P. H., SANDELL, J. H., AND MAUNSELL, J. H. R. The effect of frontal eye field and superior colliculus lesions on saccadic latencies in the rhesus monkey. *J. Neurophysiol.* 57: 1033–1049, 1987.

SCUDDER, C. A new local feedback model of the saccadic burst generator. *J. Neurophysiol.* 59: 1455–1575, 1988.

SEGRAVES, M. A. AND GOLDBERG, M. E. Functional properties of corticotectal neurons in the monkey's frontal eye field. *J. Neurophysiol.* 58: 1387–1419, 1987.

SHARPE, J. A., TROOST, B. F., DELL'OSSO, L. F., AND DAROFF, R. B. Comparative velocities of different types of fast eye movements in man. *Invest. Ophthalmol.* 14: 689–692, 1975.

SMIT, A. C. AND VAN GISBERGEN, J. A. M. A short-latency transition in saccade dynamics during square-wave tracking and its significance for the differentiation of visually-guided and predictive saccades. *Exp. Brain Res.* 76: 64–74, 1989.

SMIT, A. C., VAN GISBERGEN, J. A. M., AND COOLS, J. A parametric analysis of human saccades in different experimental paradigms. *Vision Res.* 57: 1745–1762, 1987.

SPARKS, D. L., MAYS, L. E., AND PORTER, J. D. Eye movements induced by pontine stimulation: interaction with visually triggered saccades. *J. Neurophysiol.* 58: 300–317, 1987.

STRASSMAN, A., HIGHSTEIN, S. M., AND MCCREA, R. A. Anatomy and physiology of saccadic burst neurons in the alert squirrel monkey. *J. Comp. Neurol.* 249: 337–357, 1986.

STRYKER, M. AND BLAKEMORE, C. Saccadic and disjunctive eye movements in cats. *Vision Res.* 12: 2005–2013, 1972.

TOMLINSON, R. D. AND BAHRA, P. S. Combined eye-head gaze shifts in the primate. I. Metrics. *J. Neurophysiol.* 56: 1542–1557, 1986a.

TOMLINSON, R. D. AND BAHRA, P. S. Combined eye-head gaze shifts in the primate. II. Interactions between saccades and the vestibuloocular reflex. *J. Neurophysiol.* 56: 1558–1570, 1986b.

TOMLINSON, R. D. AND ROBINSON, D. A. Signals in vestibular nucleus mediating vertical eye movements in the monkey. *J. Neurophysiol.* 51: 1121–1136, 1984.

UCHINO, Y. AND HIRAI, N. Axon collaterals of anterior semicircular canal-activated vestibular neurons and their coactivation of extraocular and neck motoneurons in the cat. *Neurosci. Res.* 1: 309–325, 1984.

VIDAL, P. P., CORVISIER, J., AND BERTHOZ, A. Eye and neck motor signals in periabducens reticular neurons of the alert cat. *Exp. Brain Res.* 53: 16–28, 1983.

VIDAL, P. P., ROUCOUX, A., AND BERTHOZ, A. Horizontal eye position-related activity in neck muscles of the alert cat. *Exp. Brain Res.* 46: 448–453, 1982.

VOLLE, M. A. *Contributions a l'etude des coordinations olculo-cephaliques chez l'homme et l'animal* (PhD thesis). Montreal, Canada: McGill Univ., 1988.

WAITZMAN, D. M., MA, T. P., OPTICAN, L. M., AND WURTZ, R. H. Superior colliculus neurons provide the saccadic motor error signal. *Exp. Brain Res.* 72: 649–652, 1988.

WHITTINGTON, D. A., HEPP-REYMOND, M. C., AND FLOOD, W. Eye and head movements to auditory targets. *Exp. Brain Res.* 41: 358–363, 1981.

YOSHIDA, K., BERTHOZ, A., VIDAL, P. P., AND MCCREA, P. Eye movement related activity of identified second order vestibular neurons in the cat. In: *Progress in Oculomotor Research,* edited by A. F. Fuchs and W. Becker. Amsterdam: Elsevier/North Holland, 1981, p. 371–378.

ZANGEMEISTER, W. H., JONES, A., AND STARK, L. Dynamics of head movement trajectories: main sequence relationship. *Exp. Neurol.* 71: 76–91, 1981.

ZANGEMEISTER, W. H. AND STARK, L. Gaze latency: variable interactions of head and eye latency. *Exp. Neurol.* 75: 389–406, 1982a.

ZANGEMEISTER, W. H. AND STARK, L. Types of gaze movement: variable interactions of eye and head movements. *Exp. Neurol.* 77: 563–577, 1982b.